

Discontinuities of free theories on AdS_2

Justin R. David^a, Edi Gava^{b,d}, Rajesh Kumar Gupta^c, K.S. Narain^d

^a*CHEP, Indian Institute of Science, C.V. Raman Avenue, Bangalore 560012, India.*

^b*INFN, sezione di Trieste, Italy.*

^c*Department of Physics, Indian Institute of Technology Ropar, Rupnagar, Punjab 140001, India.*

^d*ICTP, Strada Costiera 11, 34151 Trieste, Italy.*

E-mail: justin@iisc.ac.in, gava@ictp.it, rajesh.gupta@iitrpr.ac.in,
narain@ictp.it

ABSTRACT: The partition functions of free bosons as well as fermions on AdS_2 are not smooth as a function of their masses. For free bosons, the partition function on AdS_2 is not smooth when the mass saturates the Breitenlohner-Freedman bound. We show that the expectation value of the scalar bilinear on AdS_2 exhibits a kink at the BF bound and the change in slope of the expectation value with respect to the mass is proportional to the inverse radius of AdS_2 . For free fermions, when the mass vanishes the partition function exhibits a kink. We show that expectation value of the fermion bilinear is discontinuous and the jump in the expectation value is proportional to the inverse radius of AdS_2 . We then show the supersymmetric actions of the chiral multiplet on $AdS_2 \times S^1$ and the hypermultiplet on $AdS_2 \times S^2$ demonstrate these features. The supersymmetric backgrounds are such that as the ratio of the radius of AdS_2 to S^1 or S^2 is dialled, the partition functions as well as expectation of bilinears are not smooth for each Kaluza-Klein mode on S^1 or S^2 . Our observation is relevant for evaluating one-loop partition function in the near horizon geometry of extremal black holes.

Contents

1	Introduction	1
2	Bosons on AdS_2	3
2.1	The partition function and the kink in $\langle\phi^2\rangle$: numerics	3
2.2	The kink in $\langle\phi^2\rangle$ from AdS_2 Green's function	7
2.3	The kink in $\langle\phi^2\rangle$ from its Fourier decomposition	11
3	Fermions on AdS_2	15
3.1	The free energy and fermion bilinear: numerics	15
3.2	Fermion bilinear from the Greens function	19
4	Supersymmetric actions on $AdS_2 \times S^1$ and $AdS_2 \times S^2$	24
4.1	Chiral multiplet on $AdS_2 \times S^1$	24
4.2	Hypermultiplet on $AdS_2 \times S^2$	26
5	Conclusions	29
A	Notations and Conventions	30

1 Introduction

Near horizon geometries of extremal black holes, or BPS black holes in supersymmetric theories contain an Euclidean AdS_2 which describes the geometry of the non-compact space, see for example in [1]. Even near-extremal limit of a large class of black holes are described by a AdS_2 throat region, see for example in [2]. For both these situations it is important to study fields in the background of AdS_2 geometry. For instance in [1, 3–8] the logarithmic corrections to black hole entropy were obtained by evaluating the partition function of various fields in the background of $AdS_2 \times S^2$ which is the near horizon geometry of both BPS as well as extremal but non-supersymmetry black holes in 4 dimensions.

It has been argued that the path integral in the near horizon geometry of BPS black holes in supersymmetric theories can be evaluated exactly using the method of supersymmetric localization [9–11]. These techniques also involve evaluating one loop partition functions in the AdS_2 background. It was pointed out in [12, 13] that there are obstructions to the use of localization to evaluate partition function and has been recently emphasised in [14]. This obstruction arises due to the fact that Killing spinor grows exponentially in the radial direction of AdS_2 and maps normalizable modes to non-normalizable modes¹. Therefore the supersymmetric algebra does not close in the space of normalizable modes.

¹ AdS_2 with a non-trivial monopole background for the R symmetric admits constant Killing spinors [15]. However the AdS_2 near horizon geometries of supersymmetric black holes do not contain such monopole backgrounds.

In this paper we would like to point out another phenomenon exhibited by partition functions of theories on AdS_2 . The partition function of free bosons and fermions on AdS_2 are not smooth as a function of their masses. This phenomenon is of course also seen in partition function of free bosons or free fermions on \mathbb{R}^2 at the massless limit. However in the case of AdS_2 , we will see that physical observables like expectation value of bilinears have discontinuities which are determined by the size of AdS_2 . We will then demonstrate that this phenomenon is present in supersymmetric actions which are obtained by Kaluza-Klein reduction on $AdS_2 \times S^1$ or $AdS_2 \times S^2$. These actions contain towers of Kaluza-Klein masses which can be dialled on changing the ratio of the radii of AdS_2 and the compact space. Therefore the resultant partition functions are not smooth as a function of this ratio.

Consider the free boson ϕ on AdS_2 with mass given by

$$m^2 = -\frac{1}{4L^2} + \frac{x^2}{L^2}, \quad (1.1)$$

where L is the radius of AdS_2 and x is a parameter that can be dialled. The partition function is not smooth at $x = 0$, which is the point at which the mass saturates the Breitenlohner-Freedman bound [16, 17]. We show that scalar bilinear $\langle \phi^2 \rangle$ has a kink at $x = 0$ and the change in slope of the expectation value at $x = 0$ is proportional to $1/L$. We first study this phenomenon numerically and then use the Green's function of the boson on AdS_2 to analytically demonstrate the presence of the kink. Studying the Fourier decomposition of the Green's function along the angular direction of AdS_2 in more detail, allows us to isolate the source of the kink to the fact that the normalisable wave functions changes according across $x = 0$.

For free Fermions on AdS_2 we consider the mass given by

$$m = \frac{x}{L}. \quad (1.2)$$

We show that the partition function has a kink at $x = 0$, which is the Breitenlohner-Freedman bound for fermions in AdS [18, 19]. We then evaluate the expectation value of the fermion bilinear and show that it has a discontinuity at $x = 0$. The jump in the value of the expectation value is proportional to $1/L$. We demonstrate this discontinuity both by studying the partition function using numerics as well as analytically by examining the Green's function of the fermion in AdS_2 .

As we emphasised earlier supersymmetric field theories on AdS_2 play important role in evaluating one loop corrections to black hole entropy. In this paper we consider the simplest examples of supersymmetric theories that arise on considering near horizon geometries of BPS black holes. We first examine the case of the chiral multiplet on $AdS_2 \times S^1$, let the radius of S^1 be U . This theory was considered in [12, 13, 20] where the partition function in the presence of a background vector multiplet was evaluated using the Green's function method. To keep the discussion simple we set the background vector multiplet to zero and evaluate the partition function. We show that the supersymmetric backgrounds are such that the parameter x in (1.1) and (1.2) in the masses of the bosons and fermions depends on the Kaluza-Klein mode number on S^1 and the ratio of the radii, L/U . As this ratio is

dialled we see that the partition function is not smooth when the parameter x vanishes. The critical value of the ratio L/U for which x vanishes differs for each Kaluza-Klein mode. It is also distinct for bosons and fermions. This implies that the partition function has countably infinite points at which it is not smooth or at which the expectation values of scalar or fermion bilinears behave anomalously.

Finally we study the case of the hypermultiplet on $AdS_2 \times S^2$. This geometry occurs in all near horizon geometries of BPS supersymmetric black holes in 4 dimensions. The supersymmetric background we consider on $AdS_2 \times S^2$ involves magnetic monopole on the S^2 , expectation value of the background vector multiplet scalar as well as the auxillary scalar. We show that for each angular momentum mode on S^2 , the parameter x depends on the ratio of the radii of AdS_2 to S^2 , L/U . For the bosons of the hypermultiplet the parameter x in (1.1) which determines their mass is such that it does not vanish as the ratio is dialled for any angular momentum mode. However, for the fermions we show there exists a ratio L/U for each angular momentum mode at which x vanishes. Therefore, the partition function is not smooth and the fermion bilinear is discontinuous at these countably infinite set of points.

The paper is organised as follows. In section 2 and section 3 we study the partition function of bosons and fermions on AdS_2 as the function of their masses. In section 4 we show that supersymmetric actions of the chiral multiplet on $AdS_2 \times S^1$ and the hypermultiplet on $AdS_2 \times S^2$ are not smooth as the function of the ratio of the radii of AdS_2 and the compact space. The appendix A contains the details of the conventions and notations used in the paper. It also introduces monopole harmonics which is used to evaluate the partition functions on $AdS_2 \times S^2$.

2 Bosons on AdS_2

In this section we study the free boson partition function and the scalar bilinear as a function of the mass. We first perform the study numerically and then in section 2.2 we evaluate the expectation value of scalar bilinear using the Green's function on AdS_2 and taking the coincident limit. Finally in 2.3 we demonstrate that the presence of kink in the scalar expectation value due to the fact that there is a change in the normalizable wave function as the mass is varied. This is done using the Fourier decomposition of the Green's function.

2.1 The partition function and the kink in $\langle \phi^2 \rangle$: numerics

Consider the partition function of the free boson on AdS_2 with the following mass squared

$$m^2 = -\frac{1}{4L^2} + \frac{x^2}{L^2}. \quad (2.1)$$

Here L is the radius of AdS_2 . We will study the the free energy as a function of x , which parametrizes the deviation of the mass from the Breitenlohner-Freedman bound.. We will demonstrate that the partition function is not a smooth function in x at the Breitenlohner-Freedman bound, that is when $x = 0$. We parametrize the deviation of the mass from the

Breitenlohner-Freedman by x^2 rather than say a linearly by setting $x^2 = y$ because we wish to reproduce the Localizing action of the boson on $AdS_2 \times S^1$ as in (4.8) and examine how the partition function behaves on changing the ratio of the radius of AdS_2 to S^1 ². The action of the theory is given by

$$S = \frac{1}{2} \int d^2x \sqrt{g} (g^{\mu\nu} \partial_\mu \phi \partial_\nu \phi + m^2 \phi^2), \quad (2.2)$$

where the metric on AdS_2 is given by

$$ds^2 = L^2(dr^2 + \sinh^2 r d\theta^2). \quad (2.3)$$

The free energy of the scalar is given by

$$-\log Z = \frac{1}{2} \text{Tr} \log (-\nabla + m^2), \quad (2.4)$$

where $-\nabla$ is the scalar Laplacian on AdS_2 . It is known that the Laplacian admits δ function normalizable eigen functions which are given by [21]

$$\begin{aligned} f_{\lambda p}(r, \theta) &= \frac{1}{\sqrt{2\pi L^2}} \frac{1}{2^{|p|} |p|!} \left| \frac{\Gamma(i\lambda + \frac{1}{2} + |p|)}{\Gamma(i\lambda)} \right| e^{ip\theta} \sinh^{|p|} r \\ &\quad \times {}_2F_1(i\lambda + \frac{1}{2} + |p|, -i\lambda + \frac{1}{2} + |p|, |k| + 1, -\sinh^2 \frac{r}{2}), \\ &\quad p \in \mathbb{Z}, \quad 0 \leq \lambda < \infty. \end{aligned} \quad (2.5)$$

These functions satisfy

$$-\nabla f_{\lambda p}(r, \theta) = \frac{1}{L^2} \left(\frac{1}{4} + \lambda^2 \right). \quad (2.6)$$

To evaluate the partition function, it is convenient to examine the heat kernel

$$K(r, \theta, r', \theta'; t) = \sum_p \int d\lambda e^{-t(-\nabla + m^2)} f_{\lambda p}(r, \theta) f_{\lambda p}^*(r', \theta'). \quad (2.7)$$

For the partition function, we need to take the coincident limit and since AdS_2 is a homogenous space, we can take this point to be the origin. Now, the wave functions in (2.5) vanish at the origin for all $p \neq 0$, therefore it is sufficient to look at the $p = 0$ wave function, which is

$$f_{\lambda 0}(\eta, \theta) = \frac{1}{\sqrt{2\pi L^2}} \sqrt{\lambda \tanh(\pi\lambda)}. \quad (2.8)$$

Substituting this for the coincident limit, we obtain for the heat kernel

$$K(0; t) = \frac{1}{2\pi L^2} \int_0^\infty d\lambda \tanh(\pi\lambda) e^{-t(\frac{\lambda^2}{L^2} + \frac{x^2}{L^2})}. \quad (2.9)$$

The partition function is then given by

$$\log Z = \frac{1}{2} \int_0^\infty \frac{dt}{t} \int dr d\theta \sqrt{g} K(0; t). \quad (2.10)$$

²If we were to parametrize the mass as $m^2 = -\frac{1}{4L^2} + \frac{y}{L^2}$ with $y > 0$, the second derivative of the partition function with respect to y is singular at $y = 0$.

Here the integral over AdS_2 arises due to the fact we need to take the trace of the heat kernel to evaluate one loop determinants. Substituting the Kernel in (2.9) and performing the t integral we obtain

$$\log Z = -\frac{\text{Vol}(AdS_2)}{4\pi L^2} \int_0^\infty d\lambda \tanh(\pi\lambda) \log(\lambda^2 + x^2), \quad (2.11)$$

where we have ignored a x independent constant resulting from $\log L^2$ in the integrand. The integral over λ needs to be UV regulated which we will do subsequently. We substitute the regulated volume of AdS_2 which is given by [22, 23]

$$\text{Vol}(AdS_2) = -2\pi L^2. \quad (2.12)$$

Substituting this volume, we obtain the following result for the partition function

$$\log Z(x) = \frac{1}{2} \int_0^\infty d\lambda \lambda \tanh(\pi\lambda) \log(\lambda^2 + x^2). \quad (2.13)$$

We can regulate this partition function by first subtracting a x independent constant, which is essentially the free energy in flat space. We obtain the following free energy

$$F(x) = -\frac{1}{2} \int_0^\infty d\lambda \left[\lambda \tanh(\pi\lambda) \log(\lambda^2 + x^2) - \lambda \log(\lambda^2) \right]. \quad (2.14)$$

This integral is now logarithmically divergent in the UV. We can evaluate this integral numerically by placing a cutoff at large λ . Examining the integrand, we see that if sufficient derivatives in x are taken, there is a possibility of a divergence at $x = 0$. This divergence arises at the IR, that is at $\lambda \sim 0$ of the integrand. This is manifest if we take the derivatives inside the integral. One sees that, at sufficient high order in derivatives with respect to x at $x = 0$, the integrand diverges at $\lambda = 0$. However, to answer the question of whether the sufficient derivatives of the free energy with respect to x diverges at $x = 0$, we would need to do the integral first and then differentiate with respect to x . The reason is that we do not wish to make an apriori assumption that the order of differentiation and integration can be interchanged, after all we are interested in the delicate issue of the singular behaviour of the partition function under differentiation ³.

This question of whether the free energy is smooth can be addressed numerically. We have used Mathematica to perform the integral over λ numerically with x ranging from -0.5 to 0.5 in steps of 0.001 with a cut off on $\lambda = 1000$. We then numerically differentiated, the resulting function. The result is shown in the figure 1. Note that as anticipated the resulting function is not smooth in x , there is a kink at $x = 0$ at the 2nd derivative, and the 3rd derivative is discontinuous at this point. The results do not change on further increasing the cut off placed on λ .

From this simple analysis we observe that the partition for bosons on AdS_2 with mass given in (2.1) is not a smooth function of x . At $x = 0$, when the mass saturates the Breitenlohner-Freedman bound on AdS_2 , the 3rd derivative of the function is discontinuous.

³Though we were cautious and kept the order of differentiation to be after that of the integration, we have verified that the discontinuity in the expectation value $\langle \phi^2 \rangle$ is independent of the order of performing the differentiation.

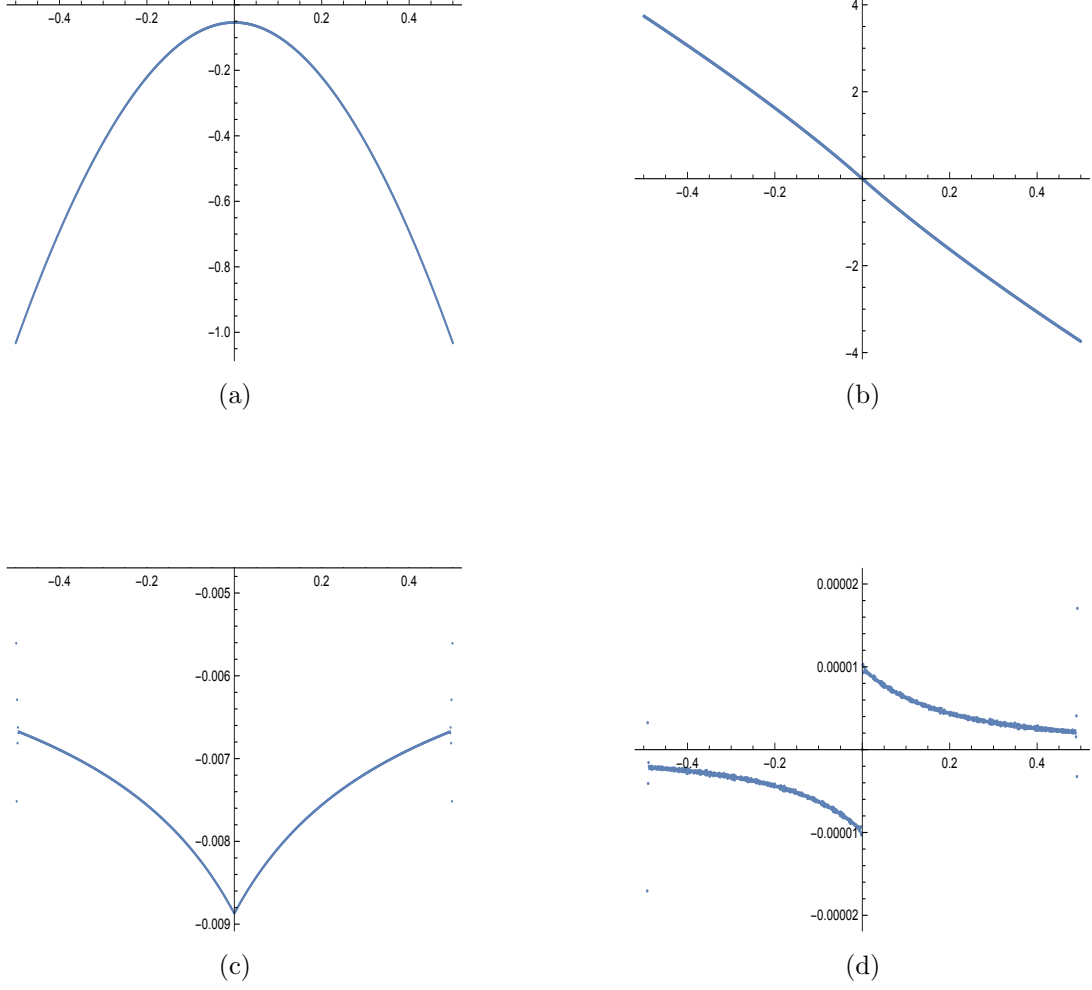


Figure 1: Plot of the Free energy given of bosons on AdS_2 given in (2.14) and its derivatives. (a) Plot of the regularized free energy $F(x)$ with respect to x . The integral is performed with a UV cut off at $\lambda = 1000$. The results do not change on further increasing this cut off. (b) Plot of $F'(x)$, (c) Plot of $F''(x)$ finally (d) Plot of $F'''(x)$

It is also instructive to study the derivative of the partition function with respect to m^2 , which is related to the integrated value of the expectation value of ϕ^2

$$-\frac{1}{2} \left\langle \int dr d\theta \sqrt{g} \phi^2(r, \theta) \right\rangle = -\frac{d}{dm^2} F(x) = -\frac{L^2}{2x} \frac{d}{dx} F(x). \quad (2.15)$$

Here we have used the action given in (2.2) and the mass in (2.1). Since AdS_2 is a homogenous space, the expectation value is independent of the position in AdS_2 . Using this and the volume of AdS_2 given in (2.12) we obtain

$$\langle \phi^2 \rangle|_{\text{numerics}} = -\frac{1}{2\pi x} \frac{d}{dx} F(x). \quad (2.16)$$

The result of evaluating this numerically is given in figure 2. This expectation value clearly shows the kink at $x = 0$ for which the mass saturates the BF bound.

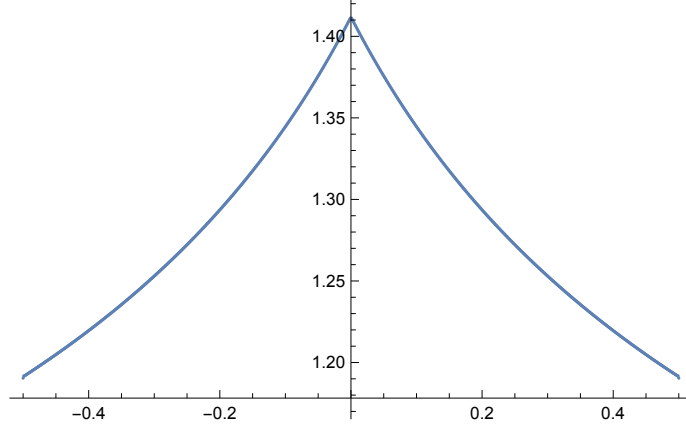


Figure 2: The expectation value of ϕ^2 given by (2.16) as a function of x obtained numerically by differentiating the free energy.

2.2 The kink in $\langle \phi^2 \rangle$ from AdS_2 Green's function

The bilinear field ϕ^2 acquires finite expectation values on AdS_2 . In section 2.1 we have used the the partition function of the scalar on AdS_2 differentiated with respect to the mass squared, m^2 and used the homogeneity of AdS_2 to obtain the expectation value. We have seen that the slope of the expectation value $\langle \phi^2 \rangle$ changes its sign at the BF bound. In this section we evaluate the change of slope analytically. The propagator on AdS_2 is known exactly. We can use the propagator and take the coincident limit to extract the expectation value of ϕ^2 on AdS_2 . We will see that though the expectation value is continuous in the variable x which determines the mass (2.1), the first derivative of the expectation value with respect to x has a discontinuity when the BF bound is saturated. We will evaluate the change of this slope analytically.

To write down the propagator on AdS_2 , it is useful to obtain the conformal dimension corresponding to the mass in (2.1). This is given by

$$\begin{aligned}\Delta &= \frac{1}{2} + \sqrt{(mL)^2 + \frac{1}{4}}, \\ &= \frac{1}{2} + |x|.\end{aligned}\tag{2.17}$$

Let us also define

$$\begin{aligned}\nu &= \sqrt{(mL)^2 + \frac{1}{4}}, \\ &= |x|.\end{aligned}\tag{2.18}$$

Note that ν vanishes when the mass of the scalar saturates the BF bound. Let us define the distance

$$\frac{1}{\xi} = \cosh r \cosh r' - \sinh r \sinh r' \cos(\theta - \theta').\tag{2.19}$$

Then the scalar Greens function of this scalar is given by [24]⁴

$$\begin{aligned}\langle \phi(r, \theta) \phi(r', \theta') \rangle &= G(\xi) = G(r, \theta, r', \theta'), \\ &= \frac{C_\Delta}{2\nu} \left(\frac{\xi}{2} \right)^\Delta F\left(\frac{\Delta}{2}, \frac{\Delta}{2} + \frac{1}{2}, \nu + 1; \xi^2 \right) \\ C_\Delta &= \frac{\Gamma(\Delta)}{\sqrt{\pi} \Gamma(\nu)}.\end{aligned}\tag{2.20}$$

Here $1/\xi = \cosh(\mu/L)$, where μ is the geodesic distance between two points on AdS_2 . The Greens function satisfies, the equation

$$-\frac{1}{\sqrt{g}} \partial_\mu \left(\sqrt{g} g^{\mu\nu} \partial_\nu G(\xi) \right) + m^2 G(\xi) = \frac{1}{\sqrt{g}} \delta(r - r') \delta(\theta - \theta').\tag{2.21}$$

Note that from this equation and the metric in (2.3), we see that the Greens function depends on the dimensionless variables, ξ and the combination $m^2 L^2$.

To obtain the expectation value $\langle \phi^2 \rangle$ we take the coincident limit and then subtract the singular term. From the expression in (2.19), we see that the coincident limit is obtained by taking $\xi \rightarrow 1$, this leads to

$$\begin{aligned}\lim_{\xi \rightarrow 1} G(\xi) &= -\frac{1}{4\pi} \left[2\gamma + \log(2) + \log(1 - \xi) + \psi\left(\frac{1}{4} + \frac{|x|}{2}\right) + \psi\left(\frac{3}{4} + \frac{|x|}{2}\right) \right] \\ &\quad + O\left[(1 - \xi) \log(1 - \xi), (1 - \xi)\right], \\ &= -\frac{1}{4\pi} \left[2\gamma - \log 2 + \log(1 - \xi) + 2\psi\left(\frac{1}{2} + |x|\right) \right] + \dots.\end{aligned}\tag{2.22}$$

In the first line of the above equation we have substituted for Δ using (2.17). To obtain the last line we have used the identity

$$\psi\left(\frac{1}{4} + \frac{|x|}{2}\right) + \psi\left(\frac{3}{4} + \frac{|x|}{2}\right) = 2\psi\left(\frac{1}{2} + |x|\right) - \log 4.\tag{2.23}$$

We can remove the term $-\frac{1}{4\pi} \log(1 - \xi)$ in (2.22), as it is singular and identify the rest of the terms to be the expectation value $\langle \phi^2 \rangle$. However this definition is subject to an shift by an arbitrary constant. To relate to the next section, we take the $\xi \rightarrow 1$ limit, by the following limit. We set $r = r'$ and then take $r \rightarrow 0$. Then

$$\lim_{r \rightarrow 0} \log(1 - \xi)|_{r=r'} = \log \left[2r^2 \sin^2 \left(\frac{\theta - \theta'}{2} \right) \right].\tag{2.24}$$

Substituting this limit in (2.22), we obtain

$$\lim_{r \rightarrow 0} G(r, \theta, r, \theta') = -\frac{1}{2\pi} \left(\gamma + \log \left[r \sin \left(\frac{\theta - \theta'}{2} \right) \right] + \psi\left(\frac{1}{2} + |x|\right) \right).\tag{2.25}$$

It is important to note that the argument of the logarithm is dimensionless since r is a dimensionless coordinate. It is clear from the metric, that if we were to re-instate the

⁴See equation (6.12) of [24]

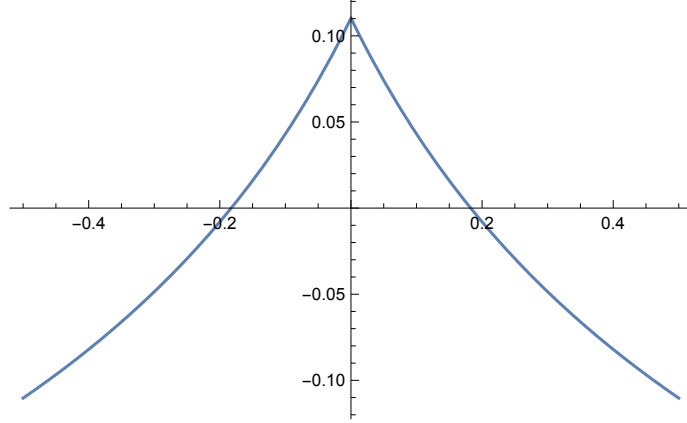


Figure 3: The expectation value of ϕ^2 given by (2.26) as a function of x .

dimensions of r , we would need to introduce the radius of AdS_2 in the logarithm. Let us identify the expectation value $\langle\phi^2\rangle$ as

$$\langle\phi^2\rangle = -\frac{1}{2\pi} \left[\gamma + \psi\left(\frac{1}{2} + |x|\right) \right]. \quad (2.26)$$

Though this identification is subject to an ambiguity by a constant, notice that the expectation value has a kink at $x = 0$, its slope is discontinuous at this point. This discontinuity is unambiguous. We have

$$\left. \frac{d}{dx} \langle\phi^2\rangle \right|_{x>0} - \left. \frac{d}{dx} \langle\phi^2\rangle \right|_{x<0} = -\frac{1}{2\pi} (\pi^2) = -\frac{\pi}{2}. \quad (2.27)$$

Note that we have determined this change in slope in units of inverse radius of AdS_2 . If we define

$$\tilde{m} = \frac{x}{L} \quad (2.28)$$

then we obtain

$$\left. \frac{d}{d\tilde{m}} \langle\phi^2\rangle \right|_{\tilde{m}>0} - \left. \frac{d}{d\tilde{m}} \langle\phi^2\rangle \right|_{\tilde{m}<0} = -\frac{1}{2\pi L} (\pi^2) = -\frac{\pi}{2L}. \quad (2.29)$$

Figure 3 contains the plot of the expectation value against x , note that this clearly shows a kink at $x = 0$. One simple consistency check for the expectation value obtain in (2.26) is the following: using (2.16) we numerically evaluated the expectation value of ϕ^2 , while in (2.26) we have evaluated the expectation value analytically using the Greens function. As we have emphasised that the definition of the expectation value is ambiguous upto a constant, therefore we must have

$$\langle\phi^2\rangle_{\text{numerics}} + A = \langle\phi^2\rangle, \quad (2.30)$$

where the left hand side of this equation is obtained by (2.16) and A is the constant which relates the two definitions. We have verified the equation (2.30) numerically and found

$A = -1.30159$. The LHS of (2.30) is plotted in figure (2), it precisely agrees with (3). The absolute value of the difference

$$\Delta = |\langle \phi^2 \rangle_{\text{numerics}} + A - \langle \phi^2 \rangle| \quad (2.31)$$

is plotted in figure (4). We see that $\Delta \leq 10^{-5}$.

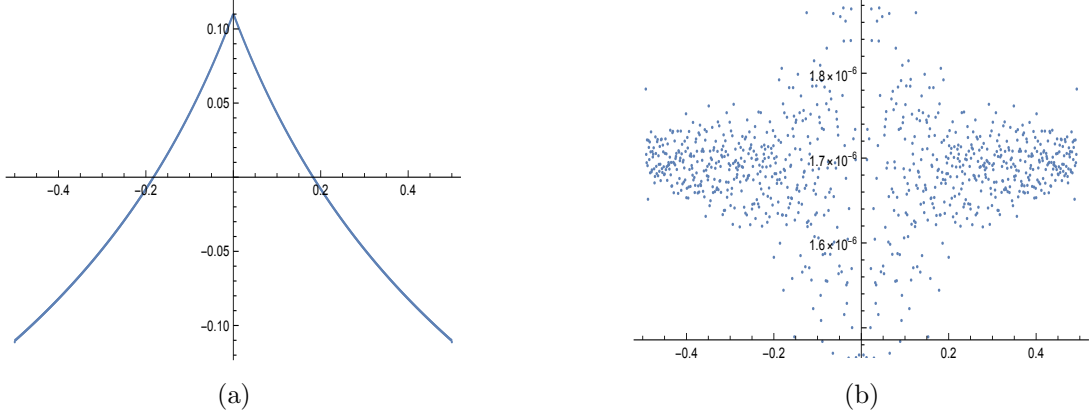


Figure 4: (a) Plot of $\langle \phi^2 \rangle_{\text{numerics}} + A$ with $A = -1.30159$ with respect to x . . Note that the graph looks identically to the one in Figure (3). (b) Plot of the difference Δ as defined in 2.31, observe that $\Delta \leq 10^{-5}$.

$\langle \phi^2 \rangle$ for the free boson on \mathbb{R}^2

At this point it is illustrative to compare the results for the expectation value of the scalar bilinear that we obtained on AdS_2 with that when one considers the free boson on flat space. The Green's function is given by

$$\begin{aligned} \langle \phi(\vec{y}) \phi(0, 0) \rangle_{\mathbb{R}^2} &= \frac{1}{4\pi^2} \int d^2 p \frac{e^{i\vec{p} \cdot \vec{y}}}{p^2 + m^2}, \\ &= \frac{1}{2\pi} K_0(m|y). \end{aligned} \quad (2.32)$$

Here $\vec{y} = (y_1, y_1)$ the co-ordinates on \mathbb{R}^2 , $y^2 = \vec{y} \cdot \vec{y}$ and K_0 refers to the modified Bessel function. To obtain the expectation value we perform the short distance expansion on the Green's function we obtain

$$\lim_{\vec{y} \rightarrow 0} \langle \phi(\vec{y}), \phi(0, 0) \rangle_{\mathbb{R}^2} = -\frac{1}{4\pi} \left(2\gamma - 2 \log 2 + \log(m^2 y^2) + O(m^2 y^2, m^2 y^2 \log(m^2 y^2)) \right). \quad (2.33)$$

We can compare this with equation (2.25), which is the result on AdS_2 . There we see that the argument of the logarithmic divergence is dimensionless and the scale which is responsible for that is the radius of AdS_2 . On \mathbb{R}_2 , the only scale is the mass. We can proceed by defining the expectation value by subtracting the logarithmic divergence just

as it was done in the AdS_2 case ⁵, we obtain

$$\langle \phi^2 \rangle_{\mathbb{R}^2} = -\frac{1}{2\pi}(\gamma - \log 2). \quad (2.34)$$

This does not have a kink, more importantly it does not have a change in slope that we saw in the AdS_2 case in (2.27) ⁶.

2.3 The kink in $\langle \phi^2 \rangle$ from its Fourier decomposition

In this section we re-examine two point function $\langle \phi(r, \theta) \phi(r', \theta') \rangle$ in terms of its Fourier decomposition along the angular direction in AdS_2 . We will see that the discontinuity in the slope of the expectation value $\langle \phi^2 \rangle$ arises solely due to the zero mode in the angular direction. As before, we parametrise the mass of the scalar as

$$m^2 = -\frac{1}{4L^2} + \frac{x^2}{L^2}, \quad (2.35)$$

therefore the Breitenlohner-Freedman bound is reached at $x = 0$. Each Fourier mode of the Green's function $\langle \phi(r, \theta) \phi(r', \theta') \rangle$ satisfies an ordinary differential equation in the radial co-ordinate r with a delta function source. The Green's function have to satisfy smoothness at the origin $r = 0$ and should be normalizable at the boundary. We will see that though the mass depends on x^2 , the choice of the normalizable wave function to construct the Green's function depends on the sign of x . The kink in the expectation value at $x = 0$ results due to the different choice of wave functions for $x > 0$ versus $x < 0$ for the zero mode along the angular direction.

To begin, the Green's function satisfies the differential equation (2.21)

$$\begin{aligned} \partial_r [\sinh r \partial_r G(r, \theta, r', \theta')] + \frac{1}{\sinh r} \partial_\theta^2 G(r, \theta, r', \theta') \\ + \frac{1}{4}(1 - 4x^2) \sinh r G(r, \theta, r', \theta') = -\delta(r - r') \delta(\theta - \theta'). \end{aligned} \quad (2.36)$$

We Fourier expand the Green's function as

$$G(r, \theta, r', \theta') = \frac{1}{2\pi} \sum_{p=-\infty}^{\infty} \hat{G}_p(r, r', p) e^{ip(\theta - \theta')}. \quad (2.37)$$

Then each Fourier mode of the Green's function satisfies the equation

$$\begin{aligned} \sinh r \partial_r^2 \hat{G}(r, r', p) + \cosh r \partial_r \hat{G}(r, r', p) - \frac{p^2}{\sinh r} \hat{G}(r, r', p) \\ + \frac{1}{4}(1 - 4x^2) \sinh r \hat{G}(r, r', p) = -\delta(r - r'). \end{aligned} \quad (2.38)$$

⁵We need to include the factor of m^2 in the logarithm since only then the argument is dimensionless for the theory on \mathbb{R}_2 .

⁶Even if the factor of m^2 was retained in the expectation value, the change in the slope of the expectation value is certainly not finite as in the case of AdS_2 seen in (2.27).

To construct the Green's function, we solve the homogenous equation. Let $\varphi_{\text{in}}(r, p)$ be the solution which is smooth at the origin and let $\varphi_{\text{out}}(r, p)$ be the solution which obeys normalizable boundary conditions as $r \rightarrow \infty$ ⁷ Then the Green's function is given by

$$\hat{G}(r, r', p) = \begin{cases} \frac{1}{W_p} \varphi_{\text{in}}(r) \varphi_{\text{out}}(r') & \text{for } r < r', \\ \frac{1}{W_p} \varphi_{\text{out}}(r) \varphi_{\text{in}}(r') & \text{for } r > r'. \end{cases} \quad (2.39)$$

Here W_p is a constant related to the Wronskian of the homogenous differential equation. By construction, the Green's function is continuous at $r = r'$. The discontinuity of the slope at $r = r'$ is obtained by integrating the equation (2.36) in this neighbourhood. This results in the equation

$$\frac{\sinh r}{W_p} \left(\frac{d\varphi_{\text{out}}(r, p)}{dr} \varphi_{\text{in}}(r, p) - \frac{d\varphi_{\text{in}}(r, p)}{dr} \varphi_{\text{out}}(r, p) \right) = -1. \quad (2.40)$$

Since we are interested in the expectation value $\langle \phi^2 \rangle$ which is obtained in the coincident limit, we can examine the solutions $\varphi_{\text{in}}(r, p), \varphi_{\text{out}}(r, p)$ as series expansions as $r \rightarrow 0$ and construct the Green's function in the coincident limit.

Non-zero modes

We will first construct the solutions for $p \neq 0$ as a series expansion in r . The smooth solutions at $r = 0$ are given by

$$\begin{aligned} \varphi_{\text{in}}(r, p) &= r^p \left(1 - \frac{1}{48(1+p)} (3 + 4p + 4p^2 - 12x^2) r^2 + \dots \right), & \text{for } p \geq 1, \\ \varphi_{\text{in}}(r, p) &= r^{-p} \left(1 - \frac{1}{48(1-p)} (3 - 4p + 4p^2 - 12x^2) r^2 + \dots \right), & \text{for } p = 1. \end{aligned} \quad (2.41)$$

To obtain W_p which is determined by (2.40) we need the solution which is normalizable at $r \rightarrow \infty$. Using uniqueness of the solution of the differential equation, we can write this solution as a linear combination of the singular solution at $r \rightarrow 0$ and an independent solution, which is smooth at $r \rightarrow 0$. From the Frobenius series expansion, these solutions

⁷These solutions behave as $e^{-(\frac{1}{2}+\delta)r}$ with $\delta > 0$ as $r \rightarrow \infty$. Such a behaviour ensures that the integral $\int dr d\theta \sqrt{\det g} \varphi^2$ is well behaved at radial infinity.

are given by

$$\begin{aligned}
\varphi_{\text{out}}(r, p) &= r^{-p} \left(1 - \frac{(3 - 4p + 4p^2 - 12x^2)}{48(1 - p)} r^2 + \dots \right) \\
&\quad + r^p C_{(p)} \ln r \left(1 - \frac{(3 + 4p + 4p^2 - 12x^2)}{48(1 + p)} r^2 + \dots \right), \quad \text{for } p > 1, \\
\varphi_{\text{out}}(r, 1) &= \frac{1}{r} \left(1 + \frac{1 + 1560x^2 - 2160x^4}{480(11 - 12x^2)} r^2 + \dots \right) \\
&\quad + r \left(\frac{4x^2 - 1}{8} \ln r + C_{(1)} \right) \left(1 - \frac{(11 - 12x^2)}{96} r^2 + \dots \right), \\
\varphi_{\text{out}}(r, p) &= r^p \left(1 - \frac{(3 + 4p + 4p^2 - 12x^2)}{48(1 + p)} r^2 + \dots \right) \\
&\quad + r^{-p} C_{(p)} \ln r \left(1 - \frac{(3 - 4p + 4p^2 - 12x^2)}{48(1 - p)} r^2 + \dots \right), \quad \text{for } p < -1, \\
\varphi_{\text{out}}(r, -1) &= \frac{1}{r} \left(1 + \frac{1 + 1560x^2 - 2160x^4}{480(11 - 12x^2)} r^2 + \dots \right) \\
&\quad + r \left(\frac{4x^2 - 1}{8} \ln r + C_{(-1)} \right) \left(1 - \frac{(11 - 12x^2)}{96} r^2 + \dots \right).
\end{aligned} \tag{2.42}$$

Here $C_{(p)}$ refer to undermined constants which can be fixed by extrapolating the normalizable solution at $r \rightarrow \infty$ to the origin. We will see that we would not need the constants $C_{(p)}$, to determine the behaviour of the Greens function as $r \rightarrow 0$. The solution to the Wronskian of the differential equation is given by

$$\sinh r \left(\frac{d\varphi_{\text{out}}(r, p)}{dr} \varphi_{\text{in}}(r) - \frac{d\varphi_{\text{in}}(r, p)}{dr} \varphi_{\text{out}}(r, p) \right) = -W_p, \tag{2.43}$$

where W_p is a constant. This constant can be fixed by examining the Wronskian at $r \rightarrow 0$. Now plugging in the solutions in (2.41) and (2.42) for $|p| \geq 1$, we obtain

$$W_p = 2|p|, \quad \text{for } |p| \geq 1, \tag{2.44}$$

Zero mode

Let us first construct the smooth solution near $r = 0$ using the Frobenius expansion This is given by

$$\varphi_{\text{in}}(r, 0) = 1 - \frac{1 - 4x^2}{16} r^2 + \dots \tag{2.45}$$

Again using the Frobenius expansion, we can write the solution which is singular at the origin, but normalizable at $r \rightarrow \infty$ as

$$\varphi_{\text{out}}(r, 0) = (C_{(0)} + \ln r) \left(1 - \frac{3 - 12x^2}{48} r^2 \right) - \left(\frac{1}{48} + \frac{x^2}{4} \right) r^2 + \dots \tag{2.46}$$

For the zero mode we would need the constant $C_{(0)}$. As we have mentioned earlier, this constant can be fixed by obtaining the solution which is normalizable at $r \rightarrow \infty$ and

extrapolating it to the origin. The homogenous differential equation can be solved exactly for $p = 0$. The two independent solutions are given by

$$y^{\frac{1}{4}(1-2x)} {}_2F_1\left(\frac{1}{4} - \frac{x}{2}, \frac{3}{4} - \frac{x}{2}; 1 - x; y\right), \quad y^{\frac{1}{4}(1+2x)} {}_2F_1\left(\frac{1}{4} + \frac{x}{2}, \frac{3}{4} + \frac{x}{2}; 1 + x; y\right), \quad (2.47)$$

where

$$y = \frac{1}{(\cosh r)^2}. \quad (2.48)$$

It is clear that the normalizable solution at $r \rightarrow \infty$ depends on the sign of x . For $x > 0$ the solution is given by

$$\varphi_{\text{out}}(r, 0)|_{x>0} = -\frac{\Gamma(\frac{1}{4} + \frac{x}{2})\Gamma(\frac{3}{4} + \frac{x}{2})}{2\Gamma(1+x)} y^{\frac{1}{4}(1+2x)} {}_2F_1\left(\frac{1}{4} + \frac{x}{2}, \frac{3}{4} + \frac{x}{2}; 1 + x; y\right). \quad (2.49)$$

Here we see that the solution behaves as

$$\lim_{r \rightarrow \infty} \varphi_{\text{out}}(r, 0) \Big|_{x>0} \sim e^{-(\frac{1}{2}+x)r}. \quad (2.50)$$

This is the required behaviour in AdS_2 for the solution to be normalizable. Expanding this solution at the origin we can determine the constant $C_{(0)}$ which is given by

$$C_{(0)}|_{x>0} = \psi\left(\frac{1}{2} + x\right) + \gamma - \log 2, \quad (2.51)$$

Note that the overall normalization for the solution in (2.49) is chosen so that the coefficient of $\log(r)$ in the $r \rightarrow 0$ limit is unity as in the Frobenius expansion (2.46). Similarly we see for $x < 0$, the normalizable solution is given by

$$\varphi_{\text{out}}(r, 0)|_{x<0} = -\frac{\Gamma(\frac{1}{4} - \frac{x}{2})\Gamma(\frac{3}{4} - \frac{x}{2})}{2\Gamma(1-x)} y^{\frac{1}{4}(1-2x)} {}_2F_1\left(\frac{1}{4} - \frac{x}{2}, \frac{3}{4} - \frac{x}{2}; 1 - x; y\right), \quad (2.52)$$

and expanding this solution at the origin we find

$$C_{(0)}|_{x<0} = \psi\left(\frac{1}{2} - x\right) + \gamma - \log 2. \quad (2.53)$$

Evaluating the proportionality constant W_0 for the Wronskian of the solutions for $p = 0$ by using their expansion at $r = 0$ we find that

$$W_0 = -1. \quad (2.54)$$

Greens function

Substituting the solutions in (2.41), (2.42), (2.47), (2.49) and value of the constant W_p (2.44), (2.54) into the expression for each mode of the Green's function given in (2.39), we

obtain the following expressions when $r = r'$ and in the small r expansion

$$\begin{aligned}
\hat{G}(r, r, p) &= \frac{1}{2p} - \frac{1 - 4x^2}{16p(1 - p^2)} r^2 + \dots, \quad p > 1 \\
\hat{G}(r, r, 1) &= \frac{1}{2} - \frac{(151 - 720x^2 + 720x^4 + (165 - 840x^2 + 720x^4) \ln r - (1320 - 1440x^2)C_{(1)})}{240(11 - 12x^2)} r^2 \\
&\quad + O(r^4), \\
\hat{G}(r, r, 0) &= -\ln r - C_0 + \frac{1}{48}(1 + 12x^2 + 6(1 - 4x^2) \ln r + 6(1 - 4x^2)C_{(0)})r^2 + \dots, \\
\hat{G}(r, r, -1) &= \frac{1}{2} - \frac{151 - 720x^2 + 720x^4 + (165 - 840x^2 + 720x^4) \ln r - (1320 - 1440x^2)C_{(-1)}}{240(11 - 12x^2)} r^2 \\
&\quad + O(r^4), \\
\hat{G}(r, r, p) &= -\frac{1}{2p} + \frac{1 - 4x^2}{16p(1 - p^2)} r^2 + \dots, \quad p < -1
\end{aligned} \tag{2.55}$$

It is clear from these expressions that the constants $C_{(p)}$ for $|p| \geq 1$ do not matter for the leading behaviour in the small r expansion. Considering the leading terms for each p (2.55), we can re-sum the Fourier coefficients

$$\lim_{r \rightarrow 0} G(r, \theta, r', \theta') = -\frac{1}{2\pi} \left(\log(2r \sin \frac{(\theta - \theta')}{2}) + C_{(0)} \right) + \dots \tag{2.56}$$

The constant $C_{(0)}$ depends on the sign of x and is given in (2.51), (2.53). Comparing (2.25) and (2.56), we see that the constant precisely agrees and removing the singular term we obtain

$$\langle \phi^2 \rangle = -\frac{1}{2\pi} \left[\gamma + \psi\left(\frac{1}{2} + |x|\right) \right]. \tag{2.57}$$

The insight we gained by doing the mode by mode analysis of the Green's function is that the discontinuity in the slope of the Green's function is entirely due to the $p = 0$ mode and the reason it occurs is because the condition that the wave function is normalizable as $r \rightarrow \infty$ depends on the sign of x , which parametrises the difference of the mass squared from the BF bound (2.35). Therefore every time the mass of the boson crosses the BF bound there is a kink in the expectation value of $\langle \phi^2 \rangle$ and its slope changes sign.

3 Fermions on AdS_2

In this section we study the partition function of fermions on AdS_2 as we vary their mass. Again we first do this numerically and then we evaluate the expectation value of the fermion bilinear by obtaining the Green's function and taking the coincident limit.

3.1 The free energy and fermion bilinear: numerics

In this section, we repeat the previous analysis in the case of a free Dirac fermion on AdS_2 . There are 2 actions we will consider, the first is that of a massive Dirac fermion

$$S_I = \int d^2x \sqrt{g} \bar{\psi} (\not{D} + m) \psi. \tag{3.1}$$

while the second action is given by

$$S_{II} = \int d^2x \sqrt{g} \bar{\psi} (\not{D} + m\gamma_t) \psi. \quad (3.2)$$

The gamma matrices are given by

$$\gamma_t = \begin{pmatrix} 1 & 0 \\ 0 & -1 \end{pmatrix}, \quad \gamma^1 = \begin{pmatrix} 0 & 1 \\ 1 & 0 \end{pmatrix}, \quad \gamma^2 = \begin{pmatrix} 0 & i \\ -i & 0 \end{pmatrix}, \quad (3.3)$$

while the vielbein are

$$e^1 = L dr, \quad e^2 = L \sinh r d\theta. \quad (3.4)$$

The direction 1, 2 correspond to directions r, θ respectively. The action S_I is the canonical Dirac action with a mass. S_{II} is the action that occurs on Kaluza-Klein reduction of fermions on $AdS_2 \times S^1$ or $AdS_2 \times S^2$ as we will see in subsequent sections. We parametrize the mass as

$$m = \frac{x}{L} \quad (3.5)$$

The BF bound for fermions is given by the condition [18, 19]⁸.

$$m^2 \geq 0. \quad (3.6)$$

We will see for both these actions (3.1), (3.2), the partition function is not smooth at $x = 0$, that is when the mass saturates the BF bound. We will also show that for S_I , the expectation value the fermion bilinear $\bar{\psi}\psi$ is discontinuous at $x = 0$, while for S_{II} , the expectation value of $\bar{\psi}\gamma_t\psi$ is discontinuous.

To evaluate the partition function it is useful to introduce the normalizable eigen functions of the Dirac operator on AdS_2 . These wave functions were constructed in [21], they are given by

$$\chi_p^\pm(\lambda) = \frac{1}{\sqrt{4\pi L^2}} \left| \frac{\Gamma(1+p+i\lambda)}{\Gamma(p+1)\Gamma(\frac{1}{2}+i\lambda)} \right| e^{i(p+\frac{1}{2})\theta} \begin{pmatrix} i \frac{\lambda}{p+1} \cosh^p \frac{r}{2} \sinh^{p+1} \frac{r}{2} {}_2F_1(p+1+i\lambda, p+1-i\lambda; p+2; -\sinh^2 \frac{r}{2}) \\ \pm \cosh^{p+1} \frac{r}{2} \sinh^p \frac{r}{2} {}_2F_1(p+1+i\lambda, p+1-i\lambda; p+1; -\sinh^2 \frac{r}{2}) \end{pmatrix}. \quad (3.7)$$

Here

$$p \in \mathbb{Z}, \quad p \geq 0, \quad 0 < \lambda < \infty \quad (3.8)$$

These eigen functions satisfy

$$\not{D}\chi_{\pm,p}(\lambda) = \pm \frac{i\lambda}{L} \chi_{\pm,p}(\lambda). \quad (3.9)$$

⁸The BF bound for fermions is independent of dimensions, see equation B.19 of [18], equation 4.3 of [19]

Similarly, to cover negative half integer quantum number along θ eigen states, we have

$$\eta_p^\pm(\lambda) = \frac{1}{\sqrt{4\pi L^2}} \left| \frac{\Gamma(1+p+i\lambda)}{\Gamma(p+1)\Gamma(\frac{1}{2}+i\lambda)} \right| e^{-i(p+\frac{1}{2})\theta} \quad (3.10)$$

$$\left(\begin{array}{c} \cosh^{p+1} \frac{r}{2} \sinh^p \frac{r}{2} {}_2F_1(p+1+i\lambda, p+1-i\lambda; p+1; -\sinh^2 \frac{r}{2}) \\ \pm i \frac{\lambda}{p+1} \cosh^p \frac{r}{2} \sinh^{p+1} \frac{r}{2} {}_2F_1(p+1+i\lambda, p+1-i\lambda; p+2; -\sinh^2 \frac{r}{2}) \end{array} \right).$$

Here too p, λ takes values as given in (3.8). These eigen functions satisfy

$$\not{D}\eta_{\pm,p}(\lambda) = \pm \frac{i\lambda}{L} \eta_{\pm,p}(\lambda). \quad (3.11)$$

Note that there exists distinct eigen functions for both positive and negative λ .

Let us examine the action S_I . Performing the path integral we obtain

$$Z_I = \text{Det}(\not{D} + m). \quad (3.12)$$

Now since the eigen values of \not{D} range over both positive and negative λ , we can see that

$$\text{Det}(\not{D} + m) = \text{Det}(\not{D} - m). \quad (3.13)$$

Therefore we can write the partition function as

$$Z_I = \sqrt{\text{Det}(-\not{D}^2 + m^2)}. \quad (3.14)$$

Therefore we consider the heat kernel

$$K_I(r, \theta, r', \theta'; t) = \sum_{p=0}^{\infty} \int_0^{\infty} d\lambda e^{-t(\frac{\lambda^2}{L^2} + \frac{x^2}{L^2})} \sum_{a=\pm} (\bar{\chi}_p^a(\lambda) \chi_p^a(\lambda) + \bar{\eta}_p^a(\lambda) \eta_p^a(\lambda)). \quad (3.15)$$

To evaluate the one loop determinant, we need to take the coincident limit of the heat kernel. Again, as AdS_2 is a homogenous space, we can take the coincident limit at the origin. The wave functions in (3.7), (3.10) have the property that only $p = 0$ is non-vanishing at $r = 0$ and

$$\sum_{a=\pm} (\bar{\chi}_0^a(\lambda) \chi_0^a(\lambda) + \bar{\eta}_0^a(\lambda) \eta_0^a(\lambda)) = \frac{1}{\pi L^2} \lambda \coth(\pi \lambda). \quad (3.16)$$

Substituting this value of the wave functions in the coincident limit of the heat kernel, we obtain

$$K_I(0; t) = \frac{1}{\pi L^2} \int_0^{\infty} d\lambda \coth(\pi \lambda) e^{-t(\frac{\lambda^2}{L^2} + \frac{x^2}{L^2})}. \quad (3.17)$$

Using this expression for the coincident heat kernel, the expression for the partition function Z_I is given by

$$\log Z_I = -\frac{1}{2\pi L^2} \int_0^{\infty} \frac{dt}{t} \int dr d\theta \sqrt{g} K(0; t). \quad (3.18)$$

Substituting the coincident limit of the kernel from (3.17), we obtain

$$\log Z_I = \frac{\text{Vol}(AdS_2)}{2\pi L^2} \int_0^\infty d\lambda \lambda \coth(\pi\lambda) \log(\lambda^2 + x^2). \quad (3.19)$$

Here we have ignored the x independent constant, substituting the regularised volume of AdS_2 and again regularising by removing the x independent free energy in flat space we obtain for the the free energy

$$F_I(x) = \int_0^\infty d\lambda \left[\lambda \coth(\pi\lambda) \log(\lambda^2 + x^2) - \lambda \log(\lambda^2) \right]. \quad (3.20)$$

We can obtain the expectation value of the bilinear $\bar{\psi}\psi$ by differentiating the free energy with respect to x

$$-\langle \int dr d\theta \sqrt{g} \bar{\psi} \psi \rangle = -L \frac{d}{dx} F_I(x). \quad (3.21)$$

Since AdS_2 is a homogenous space, we can obtain the expectation value of the fermion bilinear by factoring out the volume of AdS_2 .

$$\langle \bar{\psi} \psi \rangle = -\frac{1}{2\pi L} \frac{d}{dx} F_I(x). \quad (3.22)$$

Now let us evaluate the partition function corresponding to the action S_{II} in (3.2)

$$Z_{II} = \det(\not{D} + m\gamma_t). \quad (3.23)$$

Here we write the partition function as

$$Z_{II} = \sqrt{\det(\not{D} + m\gamma_t)^2} = \sqrt{\det(-\not{D}^2 + m^2)}. \quad (3.24)$$

Comparing (3.14) and (3.24), we see that both the partition function are identical. Therefore we have

$$F_{II}(x) = \int_0^\infty d\lambda \left[\lambda \coth(\pi\lambda) \log(\lambda^2 + x^2) - \lambda \log(\lambda^2) \right]. \quad (3.25)$$

Now from the action S_{II} we see that we can obtain the expectation value of the bilinear $\bar{\psi}\gamma_t\psi$ by differentiating with respect to x . This leads to

$$-\langle \int dr d\theta \sqrt{g} \bar{\psi} \gamma_t \psi \rangle = -L \frac{d}{dx} F_{II}(x). \quad (3.26)$$

Again using the homogeneity of AdS_2 , we obtain

$$\langle \bar{\psi} \gamma_t \psi \rangle = -\frac{1}{2\pi L} \frac{d}{dx} F_{II}(x). \quad (3.27)$$

Since the free energies of both the actions are identical, the expectation value of the bilinears $\bar{\psi}\psi$ for the theory with the action S_I is the same as that of $\bar{\psi}\gamma_t\psi$ for the theory with action S_{II} .

Let us now proceed to evaluate the free energy numerically. Since the partition function for both the actions are same, for concreteness we will use the action S_{II} . We can evaluate

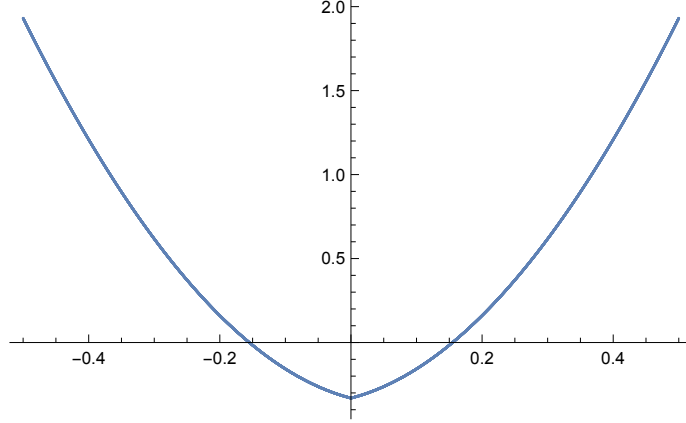


Figure 5: The free energy of fermions on AdS_2 given in (3.25) as a function of the mass parametrized by x .

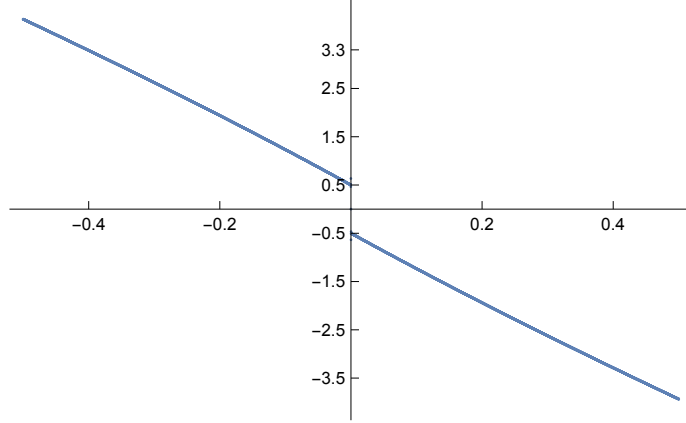


Figure 6: Expectation value $\pi L \langle \bar{\psi} \gamma_t \psi \rangle$ as function of the mass parametrized by x . Note that the expectation value is discontinuous at $x = 0$, which is the BF bound for fermions. From the graph we can read out that the jump in $\pi L \langle \bar{\psi} \gamma_t \psi \rangle$ at the BF bound is -1 .

the integral in (3.25) numerically with a cutoff at $\lambda = 1000$. We run x from -0.5 to 0.5 in steps of 0.0001 . The result is shown in figure 5, note that the plot demonstrates a kink in the free energy at the BF bound $x = 0$. Numerically differentiating the free energy using the formula in (3.27) we obtain the result shown in figure 6 which indicates that there is a jump in the expectation value of the fermion bilinear $\langle \bar{\psi} \gamma_t \psi \rangle$ at the BF bound $m = 0$. Evaluating this jump numerically we find

$$\pi L \left(\langle \bar{\psi} \gamma_t \psi \rangle|_{m \rightarrow 0^+} - \langle \bar{\psi} \gamma_t \psi \rangle|_{m \rightarrow 0^-} \right) \Big|_{\text{numerics}} = -1.005. \quad (3.28)$$

This jump can be clearly seen in the figure 6.

3.2 Fermion bilinear from the Greens function

We can compute the expectation value $\langle \bar{\psi} \gamma_t \psi \rangle$ as well as $\langle \bar{\psi} \psi \rangle$ using the Green's function of the fermion. Given the Greens's function we can use the point split approach to evaluate

these expectation values just as in the case of bosons. Therefore, let us consider the Green's function corresponding to the action (3.2). The equation of motion for the Green's function is given by

$$[(i\not{D} + m\gamma_t)G(x, x')]_{\alpha\beta} = \frac{\delta^2(x - x')}{\sqrt{g(x)}}\delta_{\alpha\beta}. \quad (3.29)$$

Here α, β refer to spinor indices. To solve for the Green's function we adapt the method of [25]. We make the following ansatz

$$G(x, x') = \left[\hat{\alpha}(\mu)\gamma_t + \hat{\beta}(\mu)n_\nu\gamma^\nu \right] \Lambda(x, x'), \quad (3.30)$$

where $\mu(x, x')$ is the geodesic distance between points x and x' given by

$$\cosh\left(\frac{\mu}{L}\right) = \frac{1}{\xi}, \quad (3.31)$$

with ξ given in (2.19). n_ν is the unit norm tangent vector at the end point x of the geodesic, defined by

$$n_\nu = D_\nu\mu(x, x'), \quad n_\mu n^\mu = 1. \quad (3.32)$$

These tangent vectors have unit norm. the details of the properties of the 'world function', $\mu(x, x')$ and its derivatives can be obtained in [26–28]. We also need the one more derivative on these tangent vectors

$$D_\nu n_\sigma = A(g_{\nu\sigma} - n_\nu n_\sigma), \quad (3.33)$$

where A is a function of μ and obeys the differential equation

$$\begin{aligned} \frac{dA}{d\mu} &= -C^2, & \frac{dC}{d\mu} &= -AC, \\ A &= \frac{1}{L} \coth\left(\frac{\mu}{L}\right), & C &= -\frac{1}{L \sinh\left(\frac{\mu}{L}\right)}. \end{aligned} \quad (3.34)$$

Finally $\Lambda(x, x')$ in (3.30) is the parallel propagator for Dirac spinors in AdS_2 , which obeys the equation

$$D_\nu \Lambda(x, x') = \frac{1}{2}(A + C)(\gamma_\nu \gamma^\sigma n_\sigma - n_\nu) \Lambda. \quad (3.35)$$

Substituting the ansatz (3.30) in the equation for the Green's function (3.29), we obtain the following equations

$$\begin{aligned} i \frac{d\hat{\alpha}}{d\mu} + \frac{i}{2}(A + C)\hat{\alpha} - m\hat{\beta} &= 0, \\ i \frac{d\hat{\beta}}{d\mu} + \frac{i}{2}(A - C)\hat{\beta} + m\hat{\alpha} &= \frac{\delta^2(x - x')}{\sqrt{g(x)}}. \end{aligned} \quad (3.36)$$

Eliminating $\hat{\beta}$, we arrive at the second order differential equation for $\hat{\alpha}$

$$\frac{d^2\hat{\alpha}}{d\mu^2} + A \frac{d\hat{\alpha}}{d\mu} - \left[\frac{C}{2}(A + C) - \frac{1}{4L^2} + m^2 \right] \hat{\alpha} = -m \frac{\delta^2(x - x')}{\sqrt{g(x)}}. \quad (3.37)$$

To solve the equation (3.37), we first observe that the first two terms are just the Laplacian acting on $\hat{\alpha}(\mu)$.

$$\begin{aligned}\partial_\nu \hat{\alpha}(\mu) &= n_\nu \frac{d\hat{\alpha}}{d\mu}, \\ D^\mu D_\mu \hat{\alpha}(\mu) &= \frac{d^2 \hat{\alpha}}{d\mu^2} + A \frac{d\hat{\alpha}}{d\mu}.\end{aligned}\tag{3.38}$$

The remaining terms in (3.37) are non-derivative terms and therefore will not affect the leading singularity near coincident points that is needed to obtain the delta function on the right hand side of (3.37). Comparing with the short distance limit the bosonic Greens function satisfies in (2.22) and its equation (2.21)⁹, we see that we must have

$$\lim_{\xi \rightarrow 1} \hat{\alpha}(\mu) = -\frac{m}{4\pi} \log(1 - \xi), \quad 1 - \xi \sim \frac{\mu^2}{2L^2}.\tag{3.39}$$

This will fix the normalization for the solution we determine. Let us change variable in the differential equation (3.37) to

$$y = \frac{1}{\cosh^2\left(\frac{\mu}{2L}\right)}.\tag{3.40}$$

Then the equation for $\hat{\alpha}$ becomes

$$y^2(1-y)\frac{d^2 \hat{\alpha}}{dy^2} - y^2 \frac{d\hat{\alpha}}{dy} - \frac{1}{4}(-1 + 4L^2 m^2 - y)\hat{\alpha} = -m \frac{\delta(r-r')\delta(\theta-\theta')}{\sinh r}.\tag{3.41}$$

Examining the corresponding homogenous equation, we obtain the following solutions

$$y^{\frac{1}{2}+Lm} {}_2F_1(Lm, 1+Lm, 1+2Lm, y), \quad y^{\frac{1}{2}-Lm} {}_2F_1(-Lm, 1-Lm, 1-2Lm, y).\tag{3.42}$$

It is clear that the normalizable solution, that is the solution which is well behaved at infinity is given by

$$\hat{\alpha}(y) = K y^{\frac{1}{2}+L|m|} {}_2F_1(L|m|, 1+L|m|, 1+2L|m|, y).\tag{3.43}$$

We can fix the constant K by examining the behaviour of the hypergeometric function at the origin $y \rightarrow 1$, which is given by

$$\lim_{y \rightarrow 1} \hat{\alpha}(y) = -K \frac{\Gamma(1+2L|m|)}{\Gamma(L|m|)\Gamma(1+L|m|)} (\log(1-y) + 2\gamma + \psi(L|m|) + \psi(1+L|m|) + \dots).\tag{3.44}$$

Here the \dots refer to terms that are suppressed at least as $(1-y)\log(1-y)$. From the definition of y in (3.40), we see that

$$\lim_{y \rightarrow 1} 1 - y = \frac{\mu^2}{4L^2} = \frac{1 - \xi}{2}.\tag{3.45}$$

To obtain the relation with ξ , we have used the equation (3.31). As we have discussed earlier, the leading behaviour if $\hat{\alpha}$ is fixed by (3.39). From (3.44) and (3.45), this implies

$$K = \frac{m}{4\pi} \frac{\Gamma(1+L|m|)\Gamma(L|m|)}{\Gamma(1+2L|m|)},\tag{3.46}$$

⁹Note that the differential equation the bosonic Green's function satisfies involves the Laplacian.

therefore

$$\hat{\alpha}(\mu) = \frac{m}{4\pi} \frac{\Gamma(1+L|m|)\Gamma(L|m|)}{\Gamma(1+2L|m|)} y^{\frac{1}{2}+L|m|} {}_2F_1(L|m|, 1+L|m|, 1+2L|m|, y). \quad (3.47)$$

We can find $\hat{\beta}(\mu)$ using the first equation of (3.36). Using this input, we obtain the following behaviour for $\hat{\alpha}$ and $\hat{\beta}$ at the coincident point

$$\begin{aligned} \lim_{\mu \rightarrow 0} \hat{\alpha}(\mu) &= -\frac{m}{4\pi} \left[\log\left(\frac{\mu^2}{4L^2}\right) + 2\gamma + \psi(L|m|) + \psi(1+L|m|) + O(\mu^2 \log \mu) \right], \\ \lim_{\mu \rightarrow 0} \hat{\beta}(\mu) &= -\frac{i}{\sqrt{2\pi}\mu} \left[1 + O(\mu^2 \log \mu) \right]. \end{aligned} \quad (3.48)$$

Now we can put all the ingredients together to obtain the behaviour of the Greens function in (3.30). Firstly the parallel propagator for the Dirac spinor obeys the equation given in (3.35). From this it is easy to see that as $\mu \rightarrow 0$, it admits a solution of the form

$$\lim_{\mu \rightarrow 0} \Lambda(x, x') = 1 - \frac{1}{8} \mu(x, x') \omega_\nu^{ab} [\gamma_a, \gamma_b] n^\nu + O(\mu^2). \quad (3.49)$$

What is important to realise from this expansion near $\mu = 0$ is that $\Lambda(x, x')$ is independent of the mass m . Consider the Green's function

$$G(x, x') = \left[\hat{\alpha}(\mu) \gamma_t + \hat{\beta}(\mu) n_\nu \gamma^\nu \right] \Lambda(x, x'). \quad (3.50)$$

We see that from relation of $\hat{\beta}$ in terms of $\hat{\alpha}$ in (3.36) and the solution of $\hat{\alpha}$ in (3.47), that $\hat{\beta}$ is a function of $|m|$. Therefore the term $\hat{\beta} n_\mu \gamma^\mu \Lambda(x, x')$ will not be discontinuous at $m = 0$. Furthermore, the finite part of this term cannot be discontinuous in its first derivative. This is because the leading singularity in $\hat{\beta}$ is a pole in μ (3.48), but whose coefficient is independent of the mass m . The pole needs to be subtracted, a finite term can arise from this pole multiplying the linear term in μ in the expansion of Λ given in (3.49) or from n_ν . But both Λ and n_μ are independent of the mass and therefore the finite term arising from the second term $\hat{\alpha}$ in the Green's function is independent of m and therefore continuous at $m = 0$.

Now let us examine the term $\hat{\alpha}(\mu) \gamma_t \Lambda(x, x')$ in the Green's function. The leading singularity in $\hat{\alpha}$ as $\mu \rightarrow 1$ is proportional to $\log(\mu)$, this is multiplied by $\Lambda(x, x')$. This singularity should be removed by the point split regularization, the finite term is therefore obtained by looking at the finite term of both $\hat{\alpha}$ and Λ in the $\mu \rightarrow 0$ limit. Therefore we can set $\Lambda = 1$ and extract the finite term from the expansion of $\hat{\alpha}$ given in (3.48). This leads to

$$\begin{aligned} \langle \bar{\psi} \gamma_t \psi \rangle &= - \lim_{\mu \rightarrow 0} \text{Tr}(\gamma_t G(x, x)) \Big|_{\text{regularised}}, \\ &= \frac{2m}{4\pi} \left[-\log(4) + 2\gamma + \psi(L|m|) + \psi(1+L|m|) \right], \end{aligned} \quad (3.51)$$

where we have regularized by subtracting the UV divergence which is proportional to $\log\left(\frac{\mu^2}{L^2}\right)$ ¹⁰. Of course this definition of the expectation value of the fermion bilinear is

¹⁰The negative sign in the first line of (3.51) is because the Greens function is defined as $G_{\alpha\beta}(x, x') = \langle \psi_\alpha(x) \bar{\psi}_\beta(x') \rangle$.

ambiguous up to a constant. Let us examine the behaviour of the following terms as $m \rightarrow 0$

$$\lim_{m \rightarrow 0} (2\gamma + \psi(L|m|) + \psi(1 + L|m|)) = -\frac{1}{L|m|} + O(L|m|). \quad (3.52)$$

Substituting this behaviour in (3.51), it is clear that the expectation value of the fermion bilinear is discontinuous at $x = 0$ and the jump in discontinuity is given by

$$\pi L \left(\langle \bar{\psi} \gamma_t \psi \rangle|_{m \rightarrow 0^+} - \langle \bar{\psi} \gamma_t \psi \rangle|_{m \rightarrow 0^-} \right) = -1. \quad (3.53)$$

We see that this agrees with the result obtained by the numerical evaluation of the partition function in (3.28). This discontinuity is not affected by the ambiguity of the constant in the definition of the expectation value in (3.51). Therefore we conclude that the fermion bilinear is $\langle \psi \gamma_t \psi \rangle$ evaluated from the partition function corresponding to the action in (3.2) is discontinuous whenever the mass of the fermion crosses the BF bound.

If one proceeds on the similar lines to evaluate the expectation value of $\bar{\psi} \psi$ for the action S_I given in (3.1) we obtain the same discontinuity. Also note from (3.53) the jump is given by $\frac{1}{\pi L}$ which vanishes in the flat space limit.

Fermion bilinear on \mathbb{R}^2

Here we evaluate the expectation of the fermion bilinear when the theory is considered on \mathbb{R}^2 . From the action (3.2), we see that the coincident limit of the fermion bilinear is given by

$$\langle \bar{\psi}(\vec{y}) \gamma_t \psi(0) \rangle_{\mathbb{R}^2} = -\frac{2}{4\pi^2} \int_{-\Lambda}^{\Lambda} dp_1 dp_2 \frac{(p_1 - m) e^{i\vec{p} \cdot \vec{y}}}{(p_1 - m)^2 + p_2^2} \quad (3.54)$$

Here we have introduced a cutoff to regulate the integral, the factor of 2 in the numerator is due to the taking the trace over the γ matrices. The coincident limit is given by

$$\langle \bar{\psi} \gamma_t \psi \rangle_{\mathbb{R}^2} = -\frac{2}{4\pi^2} \int_{-\Lambda}^{\Lambda} dp_1 dp_2 \frac{(p_1 - m)}{(p_1 - m)^2 + p_2^2} \quad (3.55)$$

It is convenient to perform the p_2 integral first ¹¹. This results in

$$\begin{aligned} \langle \bar{\psi} \gamma_t \psi \rangle_{\mathbb{R}^2} &= -\frac{1}{2\pi} \int_{-\Lambda}^{\Lambda} dp_1 \frac{p_1 - m}{|p_1 - m|}, \\ &= \frac{m}{\pi}. \end{aligned} \quad (3.56)$$

The important point to note in this result is not the value of the expectation value of the fermion bilinear which is subject to the definition of the regulator, but that it is continuous in m which is the only scale in the theory. Therefore the expectation value of the fermion bilinear on \mathbb{R}^2 does not exhibit any jumps as seen in the case of AdS_2 in (3.53).

We have performed the same analysis for the expectation value of the fermion bilinear $\langle \bar{\psi} \psi \rangle_{\mathbb{R}^2}$ with the action (3.2). The result is the same, there is no discontinuity in the expectation value at $m = 0$ contrary to what is seen for the case of AdS_2 where the discontinuity is determined by the inverse radius of AdS_2 .

¹¹The result is invariant if the p_1 integral is performed first.

4 Supersymmetric actions on $AdS_2 \times S^1$ and $AdS_2 \times S^2$

In this section we demonstrate that the supersymmetric actions one obtains by considering matter multiplets on $AdS_2 \times S^1$ or $AdS_2 \times S^2$ are such that the Kaluza-Klein masses on S^1 or S^2 can be dialled so that they saturate the BF bound. This implies, by the discussion in sections 2, 3, that the partition function of these theories are not smooth at the BF bound. Moreover expectation value of the boson bilinear have a kink and the fermion bilinear expectation value is discontinuous whenever parameters are dialled so that Kaluza-Klein masses cross the BF bound.

4.1 Chiral multiplet on $AdS_2 \times S^1$

Our first example would be the supersymmetric theory of the free chiral multiplet on the $AdS_2 \times S^1$. This has been studied in [12], where the partition function of the theory in the background of the vector multiplet was evaluated using the Greens function method. We revisit the example below but will set the vector multiplet background to zero. To connect with the discussion in the previous sections, we consider the metric of the space to be

$$ds^2 = U^2 d\tau^2 + L^2(dr^2 + \sinh^2 r d\theta^2), \quad (4.1)$$

where $\tau \in [0, 2\pi)$. The metric background together with the auxiliary fields

$$A_\tau = V_\tau = \frac{U}{L} \quad (4.2)$$

admits solutions of the killing spinor equations. For more details about the notations and the killing spinor solution, we refer to appendix A.

The supersymmetric action of free chiral multiplet on the above background is

$$S = \int d^3x \sqrt{g} \left[\mathcal{D}_\mu \bar{\phi} \mathcal{D}_\mu \phi + \left(-\frac{\Delta}{4} R + \frac{1}{2} \left(\Delta - \frac{1}{2} \right) V^2 \right) \bar{\phi} \phi + \bar{\psi} \not{D} \psi \right], \quad (4.3)$$

where

$$\begin{aligned} \mathcal{D}_\mu \phi &= \partial_\mu \phi - \frac{i}{2} (\Delta - 1) V_\mu \phi, \\ \mathcal{D}_\mu \psi &= \nabla_\mu \psi - \frac{i}{2} \Delta V_\mu \psi, \end{aligned} \quad (4.4)$$

where Δ is the R-charge of the scalar field. The Ricci scalar on AdS_2 is given by

$$R = \frac{2}{L^2} \quad (4.5)$$

Here we have incorporated the negative sign of the curvature in the curvature coupling of the action in (4.3). To see this we can set the background $V = 0$ and choose the R-charge $\Delta = \frac{1}{2}$ and observe that the action for the scalar reduces to the conformal coupled scalar on $AdS_2 \times S^1$. Let us now proceed by substituting the supersymmetric background for V_μ in (4.3) and the Ricci scalar on AdS_2 , we obtain

$$S = \int d^3x \sqrt{g} \left[\mathcal{D}_\mu \bar{\phi} \mathcal{D}_\mu \phi - \frac{1}{4L^2} \bar{\phi} \phi + \bar{\psi} \not{D} \psi \right]. \quad (4.6)$$

Next, we reduce the above action on S^1 to obtain the action on AdS_2 .

Bosons

We start with the scalar field. The expansion of the scalar in term of its Fourier modes is

$$\phi(\tau, r, \theta) = \sum_n e^{in\tau} \phi_n(r, \theta). \quad (4.7)$$

Substituting this expansion in (4.6), the action for the scalar field becomes

$$\begin{aligned} S &= \int d^3x \sqrt{g} \left[\mathcal{D}_\mu \bar{\phi} \mathcal{D}_\mu \phi - \frac{1}{4L^2} \bar{\phi} \phi \right], \\ &= 2\pi U \sum_{n=-\infty}^{\infty} \int d^2x \sqrt{\tilde{g}} \left[\tilde{g}^{ij} \partial_i \bar{\phi}_n \partial_j \phi_n + \left(\left(\frac{n}{U} - \frac{\Delta-1}{2L} \right)^2 - \frac{1}{4L^2} \right) |\phi_n|^2 \right]. \end{aligned} \quad (4.8)$$

In the above \tilde{g}_{ij} is the metric on AdS_2 of radius L . Therefore the mass of the n -th Kaluza-Klein mode is

$$m_n^2 = -\frac{1}{4L^2} + \frac{x_n^2}{L^2}, \quad \text{where} \quad x_n^2 = \left(\frac{nL}{U} - \frac{(\Delta-1)}{2} \right)^2. \quad (4.9)$$

From the discussion in section 2, we see that the partition function is not smooth whenever $x_n = 0$ or the Kaluza-Klein mass saturates the BF bound. For a given R-charge, these values are determined by the ratio of the radii of AdS_2 to S^1 , i.e., whenever the ratio is such that

$$\frac{U(\Delta-1)}{2L} \in \mathbb{Z} \quad (4.10)$$

there exists a Kaluza-Klein mass which saturates the BF bound, and therefore the partition function is not smooth as the ratio $\frac{L}{U}$ is varied. Furthermore, the expectation value

$$\langle \phi(\tau, r, \theta) \bar{\phi}(\tau, r, \theta) \rangle = \sum_{n=-\infty}^{\infty} \langle |\phi_n(r, \theta)|^2 \rangle, \quad (4.11)$$

shows a kink whenever as ratio $\frac{L}{U}$ is varied across points which satisfy (4.10).

Fermions

Similarly, let us expand the fermions in terms of Fourier modes along the S^1 direction

$$\psi(\tau, r, \theta) = \sum_n e^{i(n+r_0)\tau} \psi_n(r, \tau), \quad r_0 = 0, \text{ or } \frac{1}{2}. \quad (4.12)$$

Here, r_0 determines the periodicity of the fermion, for $r_0 = 0, \frac{1}{2}$, the fermions are periodic or anti-periodic, respectively. Substituting this expansion in the fermionic part of the action (4.6), we obtain

$$\int d^3x \sqrt{g} \bar{\psi} \not{D} \psi = 2\pi U \sum_n \int d^2x \sqrt{\tilde{g}} \left[\bar{\psi}_n \not{\tilde{D}} \psi_n + \frac{i}{L} \left(n - \frac{U\Delta}{2L} + r_0 \right) \bar{\psi}_n \gamma_1 \psi_n \right]. \quad (4.13)$$

Here $\not{\tilde{D}}$ is the covariant Dirac operator on AdS_2 . Comparing with the discussion in the section 3, we see that

$$x_n = -\left((n+r_0) - \frac{U\Delta}{2L} \right). \quad (4.14)$$

Therefore, whenever the ratio of the radii, $\frac{L}{U}$, is such that

$$\frac{U\Delta}{2L} \in \mathbb{Z} + r_0, \quad (4.15)$$

the partition function for the fermions has a kink. Furthermore, the expectation value of the fermion bilinear is given by

$$\langle \bar{\psi}(\tau, r, \theta) \gamma_1 \psi(\tau, r, \theta) \rangle = \sum_{n=-\infty}^{\infty} \langle \bar{\psi}_n(r, \theta) \gamma_1 \psi_n(r, \theta) \rangle. \quad (4.16)$$

Again from the discussion in section (3), we see that this expectation value has a discontinuity whenever the ratio of the radii satisfies (4.15).

Finally we remark that the discontinuity for the fermion in (4.15) occurs at different values of the ratio $\frac{L}{U}$ compared to that of the boson in (4.10).

4.2 Hypermultiplet on $\text{AdS}_2 \times \text{S}^2$

Our next example is the action of a free hypermultiplet on $\text{AdS}_2 \times \text{S}^2$. We consider a supersymmetric background which admits one or more killing spinor and it consists of the background metric,

$$ds^2 = L^2(dr^2 + \sinh^2 r d\theta^2) + U^2(d\varphi^2 + \sin^2 \varphi d\psi^2), \quad (4.17)$$

together with auxiliary graviphoton field $T_{\mu\nu}$ and the scalar field M . These auxiliary fields are given by

$$M = \frac{1}{L^2} - \frac{1}{U^2}, \quad T^{ab} \gamma_{ab} = -i\alpha \mathbb{I} \otimes \tau_3, \quad (4.18)$$

where $\alpha = \left(\frac{1}{4L} + \frac{1}{4U}\right)$. We follow [29] for the action of hypermultiplet and backgrounds fields. The Ricci scalar of the metric in (4.17) is given by $R = \frac{2}{L^2} - \frac{2}{U^2}$, here again we are using the positive sign for the curvature on AdS_2 and negative sign for the curvature on S^2 .

To demonstrate that the partition function of the hypermultiplet is not smooth, we also need a background vector multiplet. The vector multiplet is non-dynamical, and we choose the BPS background value, which is obtained by solving the BPS equations $\delta\lambda_i = 0$. The variation $\delta\lambda_i$ is determined by the Killing spinors on AdS_2 which is given in the appendix A. The BPS solution is

$$a_\mu = \hat{m}(1 - \cos \varphi) d\psi, \quad D_{ij} = 0, \quad \sigma = -\frac{\hat{m}}{2U}, \quad \bar{\sigma} = \frac{\hat{m}}{2U}. \quad (4.19)$$

Here \hat{m} is the magnetic flux through S^2 , D_{ij} is the auxillary field and σ is the scalar in the $\mathcal{N} = 2$ vector multiplet. The action for the free hypermultiplet is

$$\begin{aligned} \mathcal{L} = & D_\mu \phi_1^\dagger D_\mu \phi_1 + D_\mu \phi_2^\dagger D_\mu \phi_2 + \left[\frac{1}{4}(-R + M) - 4g^2 \sigma \bar{\sigma} \right] (|\phi_1|^2 + |\phi_2|^2) \\ & - \frac{i}{2} \bar{\psi} \gamma^\mu D_\mu \psi - i \bar{\psi} \gamma^{\mu\nu} \psi T_{\mu\nu} + g \bar{\psi} (\sigma P_+ + \bar{\sigma} P_-) \psi. \end{aligned} \quad (4.20)$$

Here ϕ_1 and ϕ_2 are two complex scalar fields of the hypermultiplet. The fields $\hat{\psi}$ and ψ are two 4-component Dirac spinors satisfying the reality property

$$\bar{\hat{\psi}} = \psi^\dagger, \quad \hat{\psi}^\dagger = -\bar{\psi}. \quad (4.21)$$

Also, P_\pm are projection operators that project a 4-component fermion to its positive and negative chiral part, respectively ¹². Furthermore, the covariant derivatives are

$$\begin{aligned} D_\mu \phi_1 &= (\partial_\mu - i g a_\mu) \phi_1, & D_\mu \phi_2 &= (\partial_\mu + i g a_\mu) \phi_2, \\ D_\mu \psi &= (\nabla_\mu - i g a_\mu) \psi, & D_\mu \hat{\psi} &= (\nabla_\mu + i g a_\mu) \hat{\psi}. \end{aligned} \quad (4.22)$$

Here a_μ , is the background $U(1)$ gauge field which couples to $Sp(1)$ index. We have considered only a single hypermultiplet. In principle one could consider more hypers, say r hypers. In that case this background should be thought of as turning on the gauge field in the Cartan for of $Sp(r)$.

Bosons

Next, we proceed as previously. Firstly, we start with the scalar fields. We discuss only one scalar field since both scalar fields have similar kinetic terms. We expand the scalar field in Monopole harmonics as

$$\phi_1(r, \theta, \varphi, \psi) = \sum_{\ell, p} \phi_{1g\hat{m};\ell,p}(r, \theta) Y_{g\hat{m},\ell,p}(\varphi, \psi) \quad (4.23)$$

These harmonics satisfy the following eigen value equation on S^2 .

$$\begin{aligned} -\frac{1}{U^2 \sin^2 \varphi} \left[\sin \varphi \frac{\partial}{\partial \varphi} \left(\sin \varphi \frac{\partial}{\partial \varphi} \right) + \left(\frac{\partial}{\partial \psi} - i g \hat{m} (1 - \cos \psi) \right)^2 \right] Y_{g\hat{m},\ell,p}(\varphi, \psi) \\ = \frac{\ell(\ell+1) - g^2 \hat{m}^2}{U^2} Y_{g\hat{m},\ell,p}(\varphi, \psi), \end{aligned} \quad (4.24)$$

with $\ell \geq |g\hat{m}|$. Substituting this expansion in the action for the scalar ϕ_1 , we obtain

$$\begin{aligned} \mathcal{L}_s^{(1)} &= -g^{\mu\nu} \phi_1^\dagger D_\mu D_\nu \phi_1 + \left[\frac{1}{4} (-R + M) - 4g^2 \sigma \bar{\sigma} \right] |\phi_1|^2 \\ &= -\phi_{1;g\hat{m},\ell,n}^\dagger \square_{AdS_2} \phi_{1;g\hat{m},\ell,p} + \frac{1}{U^2} \left(\ell(\ell+1) + \frac{1}{4} \left(1 - \frac{U^2}{L^2} \right) \right) \phi_{1;g\hat{m},\ell,p}^\dagger \phi_{1;g\hat{m},\ell,p} \end{aligned} \quad (4.25)$$

where \square_{AdS_2} is the Laplacian on AdS_2 , the sum over ℓ, p is implied in the second line. Note that the mass of the ℓ -the harmonic is given by

$$m_\ell^2 = \frac{4\ell(\ell+1) + 1}{U^2} - \frac{1}{4L^2}. \quad (4.26)$$

Since $\ell \geq |g\hat{m}|$, the above mass can not saturate the BF bound. Thus, the masses of the bosons in the hypermultiplet on the supersymmetric background of $AdS_2 \times S^2$ do not saturate the BF bound and therefore, we do not encounter the discontinuity in the partition function which was pointed out in section (2).

¹²We have combined the 2 Weyl spinors in the action of [29] to a Dirac spinor together with the reality constraint in (4.21).

Fermions

Next, we look at the action of fermions. From (4.20) we see that, to evaluate the one loop determinant, we need to know the eigen values of the operator \mathbb{D} where

$$\mathbb{D}\psi = \not{D}\psi + 2\gamma^{\mu\nu}T_{\mu\nu}\psi + 2ig(\sigma P_+ + \bar{\sigma}P_-)\psi. \quad (4.27)$$

Using the convention of the gamma matrices given in the appendix A, the Dirac operator appearing in the above is sum of the Dirac operator on AdS_2 and S^2 as

$$\gamma^\mu D_\mu = \mathbb{I} \otimes \not{D}_{\text{AdS}_2} + \not{D}_{S^2} \otimes \tau_3, \quad (4.28)$$

where

$$\not{D}_{\text{AdS}_2} = \frac{1}{L} \left(\frac{1}{\sinh r} \tau_1 \partial_\theta + \tau_2 \partial_r + \frac{\tau_2}{2} \coth r \right), \quad (4.29)$$

and

$$\not{D}_{S^2} = \frac{1}{U} \left(\sigma_2 \partial_\varphi + \frac{\sigma_1}{\sin \varphi} (\partial_\psi - ig a_\psi) + \frac{\sigma_2}{2} \cot \varphi \right). \quad (4.30)$$

Thus, the complete fermionic operator whose eigen values needs to be determined is given by

$$\mathbb{D}\psi = \psi_1 \otimes \not{D}_{\text{AdS}_2} \psi_2 + \not{D}_{S^2} \psi_1 \otimes \tau_3 \psi_2 - 2i\alpha \psi_1 \otimes \tau_3 \psi_2 + \frac{ig\hat{m}}{U} \sigma_3 \psi_1 \otimes \tau_3 \psi_2. \quad (4.31)$$

Here ψ_1 and ψ_2 are the two component spinors on S^2 and AdS_2 , respectively.

Next, we want to compute the eigen values of the operator \mathbb{D} . Given the eigen functions and eigen values of the Dirac operator on S^2 and AdS_2 ¹³, i.e.

$$\not{D}_{\text{AdS}_2} \psi_2 = i\zeta_1 \psi_2, \quad \not{D}_{S^2} \psi_1 = i\zeta_2 \psi_1, \quad (4.32)$$

where $\zeta_1 = \frac{\lambda}{L}$ with $\lambda \in \mathbb{R}_+$ and $\zeta_2^2 = \frac{(\ell+1)^2 - g^2 m^2}{U^2}$, it is easy to see the following relations:

$$\begin{aligned} \mathbb{D}(\psi_1 \otimes \psi_2) &= i\zeta_1 \psi_1 \otimes \psi_2 + i\zeta_2 \psi_1 \otimes \tau_3 \psi_2 - 2i\alpha \psi_1 \otimes \tau_3 \psi_2 + \frac{ig\hat{m}}{U} \sigma_3 \psi_1 \otimes \tau_3 \psi_2, \\ \mathbb{D}(\psi_1 \otimes \tau_3 \psi_2) &= -i\zeta_1 \psi_1 \otimes \tau_3 \psi_2 + i\zeta_2 \psi_1 \otimes \psi_2 - 2i\alpha \psi_1 \otimes \psi_2 + \frac{ig\hat{m}}{U} \sigma_3 \psi_1 \otimes \psi_2, \\ \mathbb{D}(\sigma_3 \psi_1 \otimes \psi_2) &= i\zeta_1 \sigma_3 \psi_1 \otimes \psi_2 - i\zeta_2 \sigma_3 \psi_1 \otimes \tau_3 \psi_2 - 2i\alpha \sigma_3 \psi_1 \otimes \tau_3 \psi_2 + \frac{ig\hat{m}}{U} \psi_1 \otimes \tau_3 \psi_2, \\ \mathbb{D}(\sigma_3 \psi_1 \otimes \tau_3 \psi_2) &= -i\zeta_1 \sigma_3 \psi_1 \otimes \tau_3 \psi_2 - i\zeta_2 \sigma_3 \psi_1 \otimes \psi_2 - 2i\alpha \sigma_3 \psi_1 \otimes \psi_2 + \frac{ig\hat{m}}{U} \psi_1 \otimes \psi_2. \end{aligned} \quad (4.33)$$

Therefore, the eigen values of the operator \mathbb{D} are obtained by finding the eigen values of the matrix

$$\begin{pmatrix} i\zeta_1 & i\zeta_2 - 2i\alpha & 0 & \frac{ig\hat{m}}{U} \\ i\zeta_2 - 2i\alpha & -i\zeta_1 & \frac{ig\hat{m}}{U} & 0 \\ 0 & \frac{ig\hat{m}}{U} & i\zeta_1 & -i\zeta_2 - 2i\alpha \\ \frac{ig\hat{m}}{U} & 0 & -i\zeta_2 - 2i\alpha & -i\zeta_1 \end{pmatrix}. \quad (4.34)$$

¹³See the appendix A for the details of the eigen functions and eigen values in the presence of the magnetic flux.

The eigen values are

$$\pm i \sqrt{\frac{\lambda^2}{L^2} + \frac{1}{U^2} \left(\ell + \frac{1}{2} - \frac{U}{2L} \right)^2}, \quad \pm i \sqrt{\frac{\lambda^2}{L^2} + \frac{1}{U^2} \left(\ell + \frac{3}{2} + \frac{U}{2L} \right)^2}, \quad (4.35)$$

where we have used the explicit form for the eigen values $\zeta_{1,2}$ and the background value of α given in (4.18). Thus, the partition function is

$$\ln Z = 4 \sum_{\ell=|gm|}^{\infty} (\ell+1) \int d\lambda \lambda \coth \pi \lambda \left[\ln \left(\frac{\lambda^2}{L^2} + \frac{1}{U^2} \left(\ell + \frac{1}{2} - \frac{U}{2L} \right)^2 \right) + \ln \left(\frac{\lambda^2}{L^2} + \frac{1}{U^2} \left(\ell + \frac{3}{2} + \frac{U}{2L} \right)^2 \right) \right] \quad (4.36)$$

Comparing with the discussion presented in the section 3, we see that the above partition function can be thought of as the partition function of Kaluza-Klein towers of fermions on AdS_2 with masses

$$m_{\ell}^{+} = \ell + \frac{3}{2} + \frac{U}{2L}, \quad m_{\ell}^{-} = \ell + \frac{1}{2} - \frac{U}{2L}. \quad (4.37)$$

In particular, we see that there is a value of the ratio of the radii of S^2 to AdS_2 , $\frac{U}{L}$ for which the mass m_{ℓ}^{-} vanishes for some ℓ . This happens when

$$\frac{U}{L} = 2\ell + 1. \quad (4.38)$$

As we have discussed in the section 3, the partition function will have a kink whenever the ratio satisfies the equation (4.38). The expectation value of the fermion bilinear will be discontinuous at these points.

5 Conclusions

The partition functions of free scalars and fermions on AdS_2 are not smooth as a function of their masses. This feature is also seen for the case of free scalars or fermions on \mathbb{R}^2 . However what is distinct in the case of AdS_2 is that the discontinuities seen in the expectation values of observables such as the scalar and fermion bilinears are determined by the inverse radius of AdS_2 . The most surprising behaviour is that of the expectation value of fermion bilinear which has a jump as the mass crosses the BF bound. The value of the jump is $-\frac{1}{\pi L}$, where L is the radius of AdS_2 .

We have shown that this anomalous behaviour of free theories on AdS_2 is exhibited in the simplest supersymmetric theories which involve AdS_2 along with compact directions. By considering supersymmetric actions, the chiral multiplet on $AdS_2 \times S^1$ and the hypermultiplet on $AdS_2 \times S^2$ we have seen these theories also exhibit the same behaviour. Here the supersymmetric backgrounds are such that the ratio of the radii of AdS_2 and the compact space plays the role of the parameter which can dial the mass. We see that discontinuities occur for each Kaluza-Klein mode.

An obvious question is whether the models in $\mathcal{N} = 2$ supergravity admitting black hole solutions with different radii of AdS_2 and S^2 exhibit this phenomenon. See [30] for a review of black hole solutions and [31] and [32] for more specific models. Therefore it is

important to derive the quadratic action of the fluctuations in the near horizon geometry of these solutions and study the behaviour of the mass spectrum.

In this paper we have focussed on AdS_2 , but the phenomenon seen here regarding discontinuities in the behaviour of free bosonic or fermionic theories should be true in higher dimensional anti-deSitter spaces. This will be interesting to study in detail further.

We have seen that key reason for the discontinuity is the fact that as the mass is dialled which of wave functions are normalisable in AdS_2 change. It will be important to examine models with interactions to see if the observation found in this paper persists. Since the discontinuity is due to the change in behaviour of the wave functions at infinity, models with interactions which do not modify this behaviour will continue to exhibit such discontinuities. Indeed we find that the model studied in [12] of the chiral multiplet coupled to a background vector also exhibits this behaviour. It will be interesting to investigate more models of supersymmetric field theories on AdS_2 together with a compact space to not only see if discontinuities in fermion bilinears persist but more importantly study its implications.

A Notations and Conventions

Conventions for $AdS_2 \times S^1$

Here we provide the conventions for the gamma matrices and the killing spinors solution on $AdS_2 \times S^2$ used in the section (4.1). Detailed discussion can be found in [12]. The covariant derivative of a fermion is given by

$$\nabla_\mu \psi = \left(\partial_\mu + \frac{i}{4} \omega_{\mu ab} \varepsilon^{abc} \gamma_c \right) \psi, \quad \varepsilon^{123} = 1. \quad (\text{A.1})$$

Our choice for 3-dimensional gamma matrices are

$$\gamma^1 = \begin{pmatrix} 1 & 0 \\ 0 & -1 \end{pmatrix}, \quad \gamma^2 = \begin{pmatrix} 0 & -1 \\ -1 & 0 \end{pmatrix}, \quad \gamma^3 = \begin{pmatrix} 0 & i \\ -i & 0 \end{pmatrix}. \quad (\text{A.2})$$

They satisfy gamma matrices algebra

$$\gamma^a \gamma^b = \delta^{ab} + i \varepsilon^{abc} \gamma_c. \quad (\text{A.3})$$

These gamma matrices are Hermitian and satisfy

$$\gamma^{aT} = -C \gamma^a C^{-1}, \quad C = \begin{pmatrix} 0 & 1 \\ -1 & 0 \end{pmatrix}, \quad C^T = -C = C^{-1}. \quad (\text{A.4})$$

Solutions of the killing spinor equations are

$$\epsilon = e^{\frac{i\theta}{2}} \begin{pmatrix} i \cosh \frac{r}{2} \\ \sinh \frac{r}{2} \end{pmatrix}, \quad \tilde{\epsilon} = e^{-\frac{i\theta}{2}} \begin{pmatrix} \sinh \frac{r}{2} \\ i \cosh \frac{r}{2} \end{pmatrix}. \quad (\text{A.5})$$

These spinors generate the killing vector given by

$$K = \frac{1}{U} \frac{\partial}{\partial \tau} + \frac{1}{L} \frac{\partial}{\partial \theta}. \quad (\text{A.6})$$

Conventions for $AdS_2 \times S^2$

Here we list the vielbeins and gamma matrices used for $AdS_2 \times S^2$ discussed in section (4.2) Vielbeins are given as

$$e^1 = L dr, \quad e^2 = L \sinh r d\theta, \quad e^3 = U d\varphi, \quad e^4 = U \sin \varphi d\psi. \quad (\text{A.7})$$

The gamma matrices are Hermitian matrix $\gamma^{\mu\dagger} = \gamma^\mu$.

$$\gamma_1 = \mathbb{I} \otimes \tau_2, \quad \gamma_2 = \mathbb{I} \otimes \tau_1, \quad \gamma_3 = \sigma_2 \otimes \tau_3, \quad \gamma_4 = \sigma_1 \otimes \tau_3. \quad (\text{A.8})$$

Here σ_i and τ_i , for $i = 1, 2, 3$ are Pauli matrices. The chiral projection operators are given by

$$P_\pm = \frac{1}{2}(1 \pm \gamma_5), \quad \text{where} \quad \gamma_5 = \gamma_1 \gamma_2 \gamma_3 \gamma_4 = -\sigma_3 \otimes \tau_3. \quad (\text{A.9})$$

The definition of the $\bar{\psi}$ is

$$\bar{\psi} = \psi^T C, \quad (\text{A.10})$$

where C is the charge conjugation matrix given by

$$C = -i\sigma_2 \otimes \tau_1. \quad (\text{A.11})$$

where σ_2 is a Pauli matrix. With the above charge conjugation matrix, the gamma matrices satisfies

$$\gamma^{\mu T} = C \gamma^\mu C^{-1}. \quad (\text{A.12})$$

The matrix $\gamma^{\mu\nu}$ is defined as

$$\gamma^{\mu\nu} = \frac{1}{2}(\gamma^\mu \gamma^\nu - \gamma^\nu \gamma^\mu). \quad (\text{A.13})$$

The killing spinor equation is given by

$$D_\mu \xi^i + \gamma^{\alpha\beta} T_{\alpha\beta} \gamma_\mu \xi^i = \gamma_\mu \eta^i, \quad (\text{A.14})$$

and the auxiliary field M is determined by the equation

$$\gamma^\mu \gamma^\nu D_\mu D_\nu \xi^i + 4\gamma^\mu D_\mu T_{ab} \gamma^{ab} \xi^i = M \xi^i. \quad (\text{A.15})$$

The spinors ξ^i are symplectic Majorana spinors satisfying the reality property

$$\xi^{i\dagger} = \epsilon_{ij} \xi^j{}^T C. \quad (\text{A.16})$$

The solutions are given by

$$\xi^1 = \frac{i}{\sqrt{2}} e^{\frac{i}{2}(\theta+\psi)} \begin{pmatrix} \sin \frac{\varphi}{2} \sinh \frac{r}{2} \\ \cosh \frac{r}{2} \sin \frac{\varphi}{2} \\ \cos \frac{\varphi}{2} \sinh \frac{r}{2} \\ \cos \frac{\varphi}{2} \cosh \frac{r}{2} \end{pmatrix}, \quad \xi^2 = \frac{i}{\sqrt{2}} e^{-\frac{i}{2}(\theta+\psi)} \begin{pmatrix} \cos \frac{\varphi}{2} \cosh \frac{r}{2} \\ \sinh \frac{r}{2} \cos \frac{\varphi}{2} \\ -\sin \frac{\varphi}{2} \cosh \frac{r}{2} \\ -\sin \frac{\varphi}{2} \sinh \frac{r}{2} \end{pmatrix}. \quad (\text{A.17})$$

These spinors generate the killing vector field given by

$$K = \frac{1}{L} \frac{\partial}{\partial \theta} - \frac{1}{U} \frac{\partial}{\partial \psi}. \quad (\text{A.18})$$

Monopoles scalar harmonics

The eigen function of the Laplace operator on unit sphere in the presence of the background magnetic flux satisfies the equation

$$-\square_{S^2} Y_{gm,\ell,p}(\varphi, \psi) = (\ell(\ell+1) - g^2 m^2) Y_{gm,\ell,p}(\varphi, \psi), \quad (\text{A.19})$$

where $\ell = |g\hat{m}|, |g\hat{m}| + 1, \dots$ and $-\ell \leq p \leq \ell$. The explicit form of the Laplace operator is

$$\square_{S^2} = \frac{1}{\sin \varphi} \partial_\varphi (\sin \varphi) + \frac{1}{\sin^2 \varphi} (\partial_\psi - ig\hat{m}(1 - \cos \varphi))^2 \quad (\text{A.20})$$

and the normalized eigen function (northern hemisphere) is

$$Y_{gm,\ell,p}(\varphi, \psi) = e^{i(p+|g\hat{m}|\psi)} \sqrt{\frac{2\ell+1}{4\pi}} \sqrt{\frac{(\ell-p)!(\ell+p)!}{(\ell+|g\hat{m}|)!(\ell-|g\hat{m}|)!}} \times \left(\cos \frac{\varphi}{2} \right)^{p-|g\hat{m}|} \left(\sin \frac{\varphi}{2} \right)^{p+|g\hat{m}|} P_{\ell-p}^{(p+|g\hat{m}|, p-|g\hat{m}|)}(\cos \varphi). \quad (\text{A.21})$$

Spinor eigen functions on AdS_2

The eigen functions of the Dirac operator on AdS_2 satisfy

$$\not{D}_{AdS_2} \chi_p^\pm(\lambda) = \pm i\lambda \chi_p^\pm(\lambda), \quad \not{D}_{AdS_2} \eta_p^\pm(\lambda) = \pm i\lambda \eta_p^\pm(\lambda). \quad (\text{A.22})$$

These are given by

$$\begin{aligned} \chi_p^\pm(\lambda) &= \frac{1}{4\pi} \left| \frac{\Gamma(1+p+i\lambda)}{\Gamma(p+1)\Gamma(\frac{1}{2}+i\lambda)} \right| e^{i(p+\frac{1}{2})\theta} \times \\ &\quad \left(\begin{aligned} &\frac{i\lambda}{p+1} \cosh^p \frac{r}{2} \sinh^{p+1} \frac{r}{2} {}_2F_1(p+1+i\lambda, p+1-i\lambda; p+2; -\sinh^2 \frac{r}{2}) \\ &\pm \cosh^{p+1} \frac{r}{2} \sinh^p \frac{r}{2} {}_2F_1(p+1+i\lambda, p+1-i\lambda; p+1; -\sinh^2 \frac{r}{2}) \end{aligned} \right), \\ \eta_p^\pm(\lambda) &= \frac{1}{4\pi} \left| \frac{\Gamma(1+p+i\lambda)}{\Gamma(p+1)\Gamma(\frac{1}{2}+i\lambda)} \right| e^{-i(p+\frac{1}{2})\theta} \times \\ &\quad \left(\begin{aligned} &\cosh^{p+1} \frac{r}{2} \sinh^p \frac{r}{2} {}_2F_1(p+1+i\lambda, p+1-i\lambda; p+1; -\sinh^2 \frac{r}{2}) \\ &\pm \frac{i\lambda}{p+1} \cosh^p \frac{r}{2} \sinh^{p+1} \frac{r}{2} {}_2F_1(p+1+i\lambda, p+1-i\lambda; p+2; -\sinh^2 \frac{r}{2}) \end{aligned} \right), \end{aligned} \quad (\text{A.23})$$

where $p \in \mathbb{Z}$, $0 \leq p < \infty$ and $0 < \ell < \infty$.

Monopole spinor harmonics

The eigen functions on S^2 in the presence of the magnetic flux satisfy

$$\not{D}_{S^2} \chi_{\ell,p}^\pm = \pm i\sqrt{(\ell+1)^2 - g^2 m^2} \chi_{\ell,p}^\pm, \quad \not{D}_{S^2} \eta_{\ell,p}^\pm = \pm i\sqrt{(\ell+1)^2 - g^2 m^2} \eta_{\ell,p}^\pm, \quad (\text{A.24})$$

Here \not{D}_{S^2} is given by

$$\not{D}_{S^2} = e_i^a \gamma^i \left(\partial_a - ig\hat{m} A_a + \frac{1}{8} \omega_{a\,ij} [\gamma^i, \gamma^j] \right), \quad (\text{A.25})$$

$a \in \{\varphi, \psi\}$ the coordinates on S^2 , i, j are the corresponding flat space indices. γ^i are the Dirac matrices and $\omega_{a ij}$ is the spin connection on S^2 . The non-zero value of the monopole vector potential is given by

$$A_\psi = \hat{m}(1 - \cos \varphi). \quad (\text{A.26})$$

The explicit form of the normalized eigen function on a S^2 in the northern hemisphere are

$$\chi_{\ell,p}^\pm = \mathcal{N} e^{i(p+g\hat{m}+\frac{1}{2})\psi} \begin{pmatrix} \pm \sqrt{\frac{\ell+1-g\hat{m}}{\ell+1+g\hat{m}}} (\cos \frac{\varphi}{2})^{p-g\hat{m}} (\sin \frac{\varphi}{2})^{1+g\hat{m}+p} P_{\ell-p}^{(1+p+g\hat{m}, p-g\hat{m})}(\cos \varphi) \\ (\cos \frac{\varphi}{2})^{1+p-g\hat{m}} (\sin \frac{\varphi}{2})^{g\hat{m}+p} P_{\ell-p}^{(p+g\hat{m}, 1+p-g\hat{m})}(\cos \varphi) \end{pmatrix}. \quad (\text{A.27})$$

The above is smooth for $\ell \geq |g\hat{m}|$ and $-g\hat{m} \leq p \leq \ell$.

$$\eta_{\ell,p}^\pm = \mathcal{N} e^{-i(p-g\hat{m}+\frac{1}{2})\psi} \begin{pmatrix} (\cos \frac{\varphi}{2})^{1+p+g\hat{m}} (\sin \frac{\varphi}{2})^{p-g\hat{m}} P_{\ell-p}^{(p-g\hat{m}, 1+p+g\hat{m})}(\cos \varphi) \\ \mp \sqrt{\frac{\ell+1+g\hat{m}}{\ell+1-g\hat{m}}} (\cos \frac{\varphi}{2})^{p+g\hat{m}} (\sin \frac{\varphi}{2})^{1+p-g\hat{m}} P_{\ell-p}^{(1+p-g\hat{m}, p+g\hat{m})}(\cos \varphi) \end{pmatrix}. \quad (\text{A.28})$$

The above exist for $g\hat{m} \leq p \leq \ell$ and $\ell \geq |g\hat{m}|$. The normalization constant is given by

$$\mathcal{N} = \sqrt{\frac{(\ell+1)}{4\pi} \frac{(\ell+p+1)!(\ell-p)!}{(\ell+g\hat{m})!(\ell-g\hat{m}+1)!}}. \quad (\text{A.29})$$

References

- [1] A. Sen, *Quantum Entropy Function from AdS_2/CFT_1 Correspondence*, *Int. J. Mod. Phys. A* **24** (2009) 4225–4244, [[0809.3304](#)].
- [2] H. K. Kunduri, J. Lucietti and H. S. Reall, *Near-horizon symmetries of extremal black holes*, *Class. Quant. Grav.* **24** (2007) 4169–4190, [[0705.4214](#)].
- [3] R. B. Mann and S. N. Solodukhin, *Universality of quantum entropy for extreme black holes*, *Nucl. Phys. B* **523** (1998) 293–307, [[hep-th/9709064](#)].
- [4] S. Banerjee, R. K. Gupta and A. Sen, *Logarithmic Corrections to Extremal Black Hole Entropy from Quantum Entropy Function*, *JHEP* **03** (2011) 147, [[1005.3044](#)].
- [5] S. Banerjee, R. K. Gupta, I. Mandal and A. Sen, *Logarithmic Corrections to $\mathcal{N} = 4$ and $\mathcal{N} = 8$ Black Hole Entropy: A One Loop Test of Quantum Gravity*, *JHEP* **11** (2011) 143, [[1106.0080](#)].
- [6] A. Sen, *Logarithmic Corrections to $N=2$ Black Hole Entropy: An Infrared Window into the Microstates*, *Gen. Rel. Grav.* **44** (2012) 1207–1266, [[1108.3842](#)].
- [7] A. Sen, *Logarithmic Corrections to Rotating Extremal Black Hole Entropy in Four and Five Dimensions*, *Gen. Rel. Grav.* **44** (2012) 1947–1991, [[1109.3706](#)].
- [8] C. Keeler, F. Larsen and P. Lisbao, *Logarithmic Corrections to $\mathcal{N} \geq 2$ Black Hole Entropy*, *Phys. Rev. D* **90** (2014) 043011, [[1404.1379](#)].
- [9] N. Banerjee, S. Banerjee, R. K. Gupta, I. Mandal and A. Sen, *Supersymmetry, Localization and Quantum Entropy Function*, *JHEP* **02** (2010) 091, [[0905.2686](#)].
- [10] A. Dabholkar, J. Gomes and S. Murthy, *Quantum black holes, localization and the topological string*, *JHEP* **06** (2011) 019, [[1012.0265](#)].

- [11] A. Dabholkar, J. Gomes and S. Murthy, *Localization & Exact Holography*, *JHEP* **04** (2013) 062, [[1111.1161](#)].
- [12] J. R. David, E. Gava, R. K. Gupta and K. Narain, *Boundary conditions and localization on AdS. Part I*, *JHEP* **09** (2018) 063, [[1802.00427](#)].
- [13] J. R. David, E. Gava, R. K. Gupta and K. Narain, *Boundary conditions and localization on AdS. Part II. General analysis*, *JHEP* **02** (2020) 139, [[1906.02722](#)].
- [14] A. Sen, *Revisiting localization for BPS black hole entropy*, [2302.13490](#).
- [15] A. Pittelli, *Supersymmetric localization of refined chiral multiplets on topologically twisted $H^2 \times S^1$* , *Phys. Lett. B* **801** (2020) 135154, [[1812.11151](#)].
- [16] P. Breitenlohner and D. Z. Freedman, *Positive Energy in anti-De Sitter Backgrounds and Gauged Extended Supergravity*, *Phys. Lett. B* **115** (1982) 197–201.
- [17] P. Breitenlohner and D. Z. Freedman, *Stability in Gauged Extended Supergravity*, *Annals Phys.* **144** (1982) 249.
- [18] A. J. Amsel and D. Marolf, *Supersymmetric Multi-trace Boundary Conditions in AdS*, *Class. Quant. Grav.* **26** (2009) 025010, [[0808.2184](#)].
- [19] O. J. C. Dias, R. Masachs, O. Papadoulaki and P. Rodgers, *Hunting for fermionic instabilities in charged AdS black holes*, *JHEP* **04** (2020) 196, [[1910.04181](#)].
- [20] J. R. David, E. Gava, R. K. Gupta and K. Narain, *Localization on $AdS_2 \times S^1$* , *JHEP* **03** (2017) 050, [[1609.07443](#)].
- [21] R. Camporesi and A. Higuchi, *Spectral functions and zeta functions in hyperbolic spaces*, *J. Math. Phys.* **35** (1994) 4217–4246.
- [22] H. Casini, M. Huerta and R. C. Myers, *Towards a derivation of holographic entanglement entropy*, *JHEP* **05** (2011) 036, [[1102.0440](#)].
- [23] I. R. Klebanov, S. S. Pufu, S. Sachdev and B. R. Safdi, *Renyi Entropies for Free Field Theories*, *JHEP* **04** (2012) 074, [[1111.6290](#)].
- [24] E. D’Hoker and D. Z. Freedman, *Supersymmetric gauge theories and the AdS / CFT correspondence*, in *Theoretical Advanced Study Institute in Elementary Particle Physics (TASI 2001): Strings, Branes and EXTRA Dimensions*, pp. 3–158, 1, 2002, [hep-th/0201253](#).
- [25] W. Mueck, *Spinor parallel propagator and Green’s function in maximally symmetric spaces*, *J. Phys. A* **33** (2000) 3021–3026, [[hep-th/9912059](#)].
- [26] J. L. Synge, ed., *Relativity: The General theory*. 1960.
- [27] P. C. Peters, *Covariant electromagnetic potentials and fields in friedmann universes*, *Journal of Mathematical Physics* **10** (1969) 1216–1224, [<https://doi.org/10.1063/1.1664961>].
- [28] B. Allen and T. Jacobson, *Vector Two Point Functions in Maximally Symmetric Spaces*, *Commun. Math. Phys.* **103** (1986) 669.
- [29] N. Hama and K. Hosomichi, *Seiberg-Witten Theories on Ellipsoids*, *JHEP* **09** (2012) 033, [[1206.6359](#)].
- [30] A. Zaffaroni, *AdS black holes, holography and localization*, *Living Rev. Rel.* **23** (2020) 2, [[1902.07176](#)].

- [31] D. Cassani, P. Koerber and O. Varela, *All homogeneous $\mathcal{N} = 2$ M-theory truncations with supersymmetric AdS_4 vacua*, *JHEP* **11** (2012) 173, [[1208.1262](#)].
- [32] N. Halmagyi, M. Petrini and A. Zaffaroni, *BPS black holes in AdS_4 from M-theory*, *JHEP* **08** (2013) 124, [[1305.0730](#)].